



2

NAVAL POSTGRADUATE SCHOOL

Monterey, California



75 PJ
B

94-09084



DTIC

ELECTE

MAR 25 1994

E

D

**ESTIMATING SUBPYCNOCLINE DENSITY FLUCTUATIONS
IN THE CALIFORNIA CURRENT REGION
FROM UPPER OCEAN OBSERVATIONS**

Robert L. Haney
Robert A. Hale
Department of Meteorology

Curtis A. Collins
Department of Oceanography

February 1994

Approved for Public Release, Distribution Unlimited

Prepared for:
Chief of Naval Research
Ballston Tower One
800 N. Quincy St.
Arlington, VA 22217-5660

94 3 22 046

Naval Postgraduate School
Monterey, California 93943-5114


Rear Admiral T. A. Mercer
Superintendent


H. Shull
Provost

This report was prepared for and funded by Office of Naval Research, Applied Research and Technology Division.

Reproduction of all or part of the report is authorized.

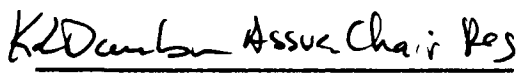
This report was prepared by:

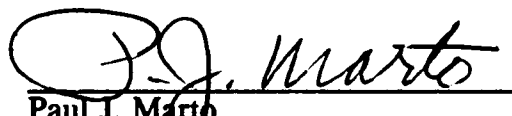

Robert L. Haney
Professor of Meteorology


Curtis A. Collins
Professor of Oceanography

Reviewed by:

Released by:


Robert L. Haney, Chairman
Department of Meteorology


Paul J. Marto
Dean of Research

REPORT DOCUMENTATION PAGE				Form Approved OMB No 0704-0188	
1a REPORT SECURITY CLASSIFICATION UNCLASSIFIED			1b RESTRICTIVE MARKINGS		
2a SECURITY CLASSIFICATION AUTHORITY			3. DISTRIBUTION/AVAILABILITY OF REPORT		
2b DECLASSIFICATION/DOWNGRADING SCHEDULE					
4. PERFORMING ORGANIZATION REPORT NUMBER(S) NPS-MR-94-001			5. MONITORING ORGANIZATION REPORT NUMBER(S)		
6a NAME OF PERFORMING ORGANIZATION Naval Postgraduate School Department of Meteorology		6b OFFICE SYMBOL (If applicable) MR	7a NAME OF MONITORING ORGANIZATION		
6c. ADDRESS (City, State, and ZIP Code) 589 Dyer Rd., Room 254 Monterey, CA 93943-5114			7b ADDRESS (City, State, and ZIP Code)		
8a NAME OF FUNDING/SPONSORING ORGANIZATION Chief of Naval Research		8b OFFICE SYMBOL (If applicable) Code 01122	9 PROCUREMENT INSTRUMENT IDENTIFICATION NUMBER N0001493WR22033		
8c. ADDRESS (City, State, and ZIP Code) Ballston Tower One 800 N. Quincy Street Arlington, VA 22217-5660			10 SOURCE OF FUNDING NUMBERS		
			PROGRAM ELEMENT NO 0601153N	PROJECT NO BR031- 03-01	TASK NO
11 TITLE (Include Security Classification) Estimating Subpynocline Density Fluctuations in the California Current Region from Upper Ocean Observations (U)					
12. PERSONAL AUTHOR(S) Robert L. Haney, Robert A. Hale, and Curtis A. Collins					
13a. TYPE OF REPORT Technical		13b TIME COVERED FROM 10/1/92 TO 9/30/93		14 DATE OF REPORT (Year, Month, Day) 1994 Feb 7	
15 PAGE COUNT					
16 SUPPLEMENTARY NOTATION					
17. COSATI CODES			18. SUBJECT TERMS (Continue on reverse if necessary and identify by block number)		
FIELD	GROUP	SUB-GROUP	California Current, Vertical Empirical Orthogonal Function (EOF) Analysis		
19 ABSTRACT (Continue on reverse if necessary and identify by block number) A method for extending upper ocean density observations to the deep ocean is tested using a large number of deep CTD stations in the California Current. The specific problem considered is that of constructing the best estimate for the density profile below a certain depth, D, given an observed profile above that depth. For this purpose, the estimated disturbance profile is modeled as a weighted sum of empirical vertical modes (EOFs). The EOFs were computed from the surface to 2000 m using 126 largely independent CTD stations off Pt. Sur, California. Separate computations were made for the summer half-year (mid-April to mid-October) and the winter half-year (mid-October to mid-April). For each observed density profile, the EOF weights that determine the estimated profile were obtained by performing a successive least squares fit of the disturbance density profile above D to the first N EOFs. In this study, N was taken to be 7, which is					
20. DISTRIBUTION/AVAILABILITY OF ABSTRACT <input checked="" type="checkbox"/> UNCLASSIFIED/UNLIMITED <input type="checkbox"/> SAME AS RPT <input type="checkbox"/> DTIC USERS			21. ABSTRACT SECURITY CLASSIFICATION UNCLASSIFIED		
22a NAME OF RESPONSIBLE INDIVIDUAL Robert L. Haney			22b TELEPHONE (Include Area Code) 408-656-2517		22c OFFICE SYMBOL MR

19. Abstract (continued)

the number of EOFs considered necessary to account for the "signal" in the profiles as determined by the methods of Preisendorfer et al. (1981) and Smith et al. (1985). The estimated profiles were then verified against the observed profiles to 2000 m, and the results are presented as a function of the depth D.

In general, the vertical extension method is moderately successful at estimating density fluctuations at and below 500 m from data entirely above 500 m. For example, if data from the upper 300 m is used, the correlation between the estimated and observed profiles at 500 m is .65 in summer and .75 in winter while the correlation at 1000 m is .40 in summer and .50 in winter. The correlations between the estimated profiles and a 7-mode reconstruction of the observed profiles, representing the observed "signal", are somewhat higher. A practical result of this study is that data down to only 200 m, as might be acquired by a SEASOR CTD survey, can estimate the "signal" part of the density fluctuations at 500 m with a correlation of .47 in summer and .69 in winter.

Table of Contents

Abstract

1.	Introduction	4
2.	The Vertical Extension Method	5
3.	The POST CTD Data	7
4.	Results of Vertical Extension	27
5.	Summary and Conclusions	65
	References	68
	Distribution List	70

Accession For	
NTIS CRA&I	<input checked="" type="checkbox"/>
DTIC TAB	<input type="checkbox"/>
Unannounced	<input type="checkbox"/>
Justification	
By	
Distribution /	
Availability Codes	
Dist	Avail and / or Special
A-1	

ABSTRACT

A method for extending upper ocean density observations to the deep ocean is tested using a large number of deep CTD stations in the California Current. The specific problem considered is that of constructing the best estimate for the density profile below a certain depth, D , given an observed profile above that depth. For this purpose, the estimated disturbance profile is modeled as a weighted sum of empirical vertical modes (EOFs). The EOFs were computed from the surface to 2000 m using 126 largely independent CTD stations off Pt. Sur, California. Separate computations were made for the summer half-year (mid-April to mid-October) and the winter half-year (mid-October to mid-April). For each observed density profile, the EOF weights that determine the estimated profile were obtained by performing a successive least squares fit of the disturbance density profile above D to the first N EOFs. In this study, N was taken to be 7, which is the number of EOFs considered necessary to account for the "signal" in the profiles as determined by the methods of Preisendorfer *et al.* (1981) and Smith *et al.* (1985). The estimated profiles were then verified against the observed profiles to 2000 m, and the results are presented as a function of the depth D .

In general, the vertical extension method is moderately successful at estimating density fluctuations at and below 500 m from data entirely above 500 m. For example, if data from the upper 300 m is used, the correlation between the estimated and observed profiles at 500 m is .65 in summer and .75 in winter while the correlation at 1000 m is .40 in summer and .50 in winter. The correlations between the estimated profiles and a 7-mode reconstruction of the observed profiles, representing the observed "signal", are

somewhat higher. A practical result of this study is that data down to only 200 m, as might be acquired by a SEASOAR CTD survey, can estimate the "signal" part of the density fluctuations at 500 m with a correlation of .47 in summer and .69 in winter.

1. Introduction

A classic problem in synoptic ocean analysis is that of estimating the deep ocean density structure from observations in the upper ocean alone. The problem is of general interest simply because there are far more observations in the upper ocean than in the deep ocean. In addition, new ocean instruments and measuring devices such as SEASOAR now make it possible to carry out hydrographic surveys of the oceanic mesoscale that are nearly synoptic in time. This is possible, however, only if the measurements are restricted to rather shallow depth ranges, e.g., the upper 200 m. The extent to which such an upper ocean survey can adequately describe the dynamical features in and below the pycnocline at a given time is therefore an important question. Subpycnocline density fluctuations on synoptic scales are important in their own right, and they also influence the dynamics of the pycnocline and upper ocean itself. For example, if hydrographic data from the upper ocean is utilized in a numerical model, the extension of the data to the deeper ocean is critical. The resulting subpycnocline density fluctuations influence the upper ocean currents through the hydrostatic and geostrophic constraints, and they exert a strong influence on subsequent model predictions (Hurlburt *et al.* 1990).

A number of recent studies have been directed at various aspects of this problem. For example, Smith *et al.* (1985) evaluated the skill with which the amplitude of quasi-geostrophic dynamical modes (which have important signals at mid-ocean depths) could be estimated from mixed CTD/XBT surveys in the California Current system. For shallow CTD and XBT casts (< 750 m), the best results were obtained using a method based on the covariances between the quasi-geostrophic modal amplitudes and the amplitudes of the first

few empirical vertical modes. Another approach for specifying density disturbances in the deeper ocean from upper ocean observations involves the use of feature models, which are relationships between sea surface temperature patterns and subsurface thermal features developed for the Gulf Stream and its warm and cold core rings (Robinson *et al.* 1988). Yet another approach is the use of statistical relations between sea level and subsurface temperature or pressure anomalies determined from numerical model simulations (Hurlburt *et al.* 1990; Mellor and Ezer 1991). These studies have shown that fluctuations in model sea level are highly correlated with fluctuations in model density at depths of 1-2 km.

In the present study, we test an empirical method which in some ways represents an observation-based generalization of the feature model approach. The method consists of fitting a disturbance density profile observed in the upper ocean to empirical vertical modes (EOFs) determined from historical CTD data taken in the region of interest. The vertical EOFs, which extend from the surface to the deep ocean, thereby represent a set of "feature models" in this method. The method is potentially useful for real-time ocean analysis and for initializing numerical ocean prediction models.

2. The Vertical Extension Method

The problem being considered is that of constructing the best estimate for the density profile below a certain depth D , given the observed density profile above that depth. As described in detail below, the estimated disturbance density profile is modeled as a weighted sum of the first N empirical vertical modes. To begin the estimation procedure, the potential density, Θ , is expressed in terms of a mean part, $\bar{\Theta}(z)$, and a disturbance part, $\Theta'(z)$,

$$\Theta(z) = \bar{\Theta}(z) + \Theta'(z), \quad (2.1)$$

and Θ' is modeled as a weighted sum of the first N vertical EOFs. Denoting the estimated profile by $\hat{\Theta}(z)$,

$$\hat{\Theta}(z) = \sum_{i=1}^N A_i \Theta_i(z), \quad (2.2)$$

where $\Theta_i(z), i=1 \dots N$, are the EOFs and A_i are their amplitudes (weights). The A_i are obtained by performing a successive least-squares fit of Θ' to the first N vertical empirical modes above the depth D . Thus, performing least-squares fit of Θ' to the first mode determines A_1 ,

$$A_1 = \frac{\langle \Theta' \Theta_1 \rangle}{\langle \Theta_1 \Theta_1 \rangle}, \quad (2.3)$$

where $\langle \rangle$ represents a vertical integral (numerical sum) from the surface to D . Performing a least-squares fit of the residual profile, $\Theta' - A_1 \Theta_1$, to the second mode determines A_2 ,

$$A_2 = \frac{\langle (\Theta' - A_1 \Theta_1) \Theta_2 \rangle}{\langle \Theta_2 \Theta_2 \rangle}, \quad (2.4)$$

and so forth up to A_N . The solutions for the A_i then determine the estimated profile, $\hat{\Theta}(z)$, through (2.2). In the following section the method is tested using a large number of deep CTD stations off Pt. Sur, California.

3. The POST CTD Data

The CTD data used in this study were collected as part of the Point Sur Transect (POST) program (Tisch *et al.* 1992). The observation site extends from 20 km to about 250 km offshore of Pt. Sur, California near 36°N (Fig. 1). All of the CTD stations were taken in water depths greater than 2000 m, and most of them were taken seaward of the region of strong coastal upwelling next to the coast. Table 1 gives a summary of all of the data which was taken approximately every two months during the three year period from April 1988 through April 1991. Details of the quality control and processing of the raw CTD data to compute the density perturbation^c used in the following analysis can be found in Tisch *et al.* (1992).

Since the goal of this study is to present regional EOFs, and to use them to test a vertical extension method, we have tried to estimate the statistical significance of our computations in several ways. First, we utilize an *a priori* knowledge of the annual variability in the region by considering two halves of the year separately. One half-year runs from mid-April to mid-October, hereafter referred to as the upwelling or summer season, and the other half-year runs from mid-October through mid-April, hereafter referred to as the winter season. With this choice, all of the POST cruises assigned to the upwelling season occurred after the well known spring transition which occurs each year near the end of March in this region (Strub *et al.* 1987; Lentz 1987). Because the stations are spaced close together, it is clear that not all of the CTD casts from a single cruise can be considered independent. In order to retain as large a sample of CTDs as possible, and at the same time to remove some of the redundancy caused by the station spacing, we culled

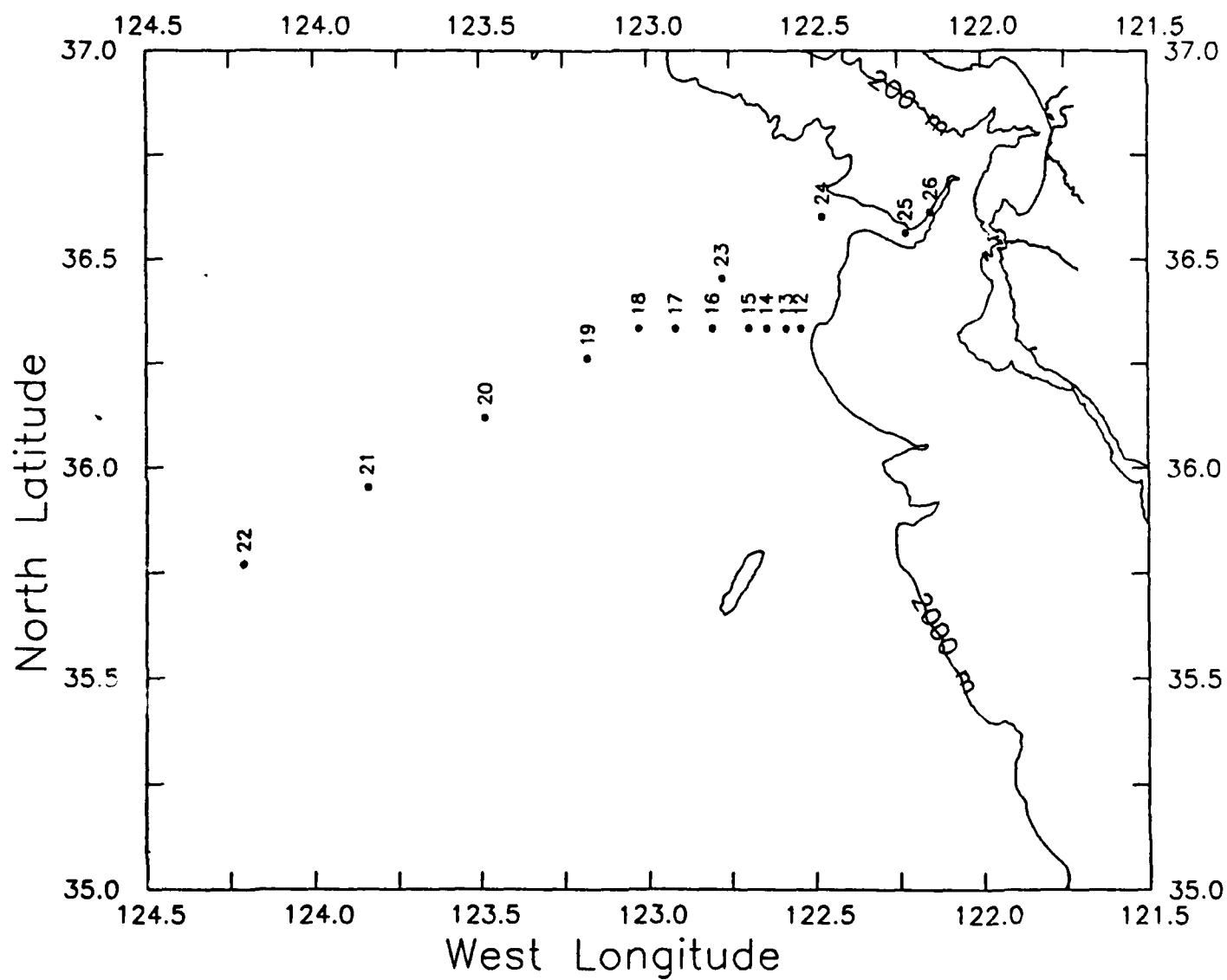


Fig. 1. Location of the POST CTD stations used in this study.

out neighboring CTD stations that had an overall correlation greater than 0.5 with a station previously selected for analysis. With this screening procedure, approximately half the stations were culled out (see Table 1). As a result, the number of profiles selected for analysis was $ND = 64$ in summer and $ND = 62$ in winter, and the average spacing between selected stations was about 25 km. We thereby feel rather comfortable in applying standard statistical techniques to the data. As a partial check on the robustness of our results, the vertical extension method was also evaluated using the culled CTDs (the ones not used to compute the EOFs). However, unless stated otherwise, all the analysis shown below is based on the screened data.

Fig. 2 shows the potential density (a) and the buoyancy frequency (b) from the surface to 2000 m, for both the summer and winter halves of the year. The stratification associated with the mean pycnocline occurs in the upper 300 - 500 m, with the maximum stratification near 60 m depth. The annual variation is rather small and confined to above 100 m where the water is less dense and more stratified in summer than in winter. As noted earlier, the study area is located seaward of the narrow upwelling zone immediately next to the coast and therefore it experiences a typical, but weak, annual cycle.

The density EOFs are shown in Fig. 3. The statistical significance of the EOF shapes was estimated using an eigenvalue method (North *et al.* 1982) and a bootstrap method (Smith 1984; Smith *et al.* 1985). In the eigenvalue method, one compares the sampling error, $\delta \lambda$, of a particular eigenvalue λ , $\delta \lambda \sim \lambda \sqrt{2/ND}$, to the spacing $\Delta \lambda$, between λ and a neighboring eigenvalue (North *et al.* 1982). The shape of the EOF corresponding to λ is statistically significant only if $\delta \lambda < \Delta \lambda$ holds for both neighboring eigenvalues of λ . The

Table 1. Dates of the POST cruises from which the CTD data for this study were taken. Of the 250 total CTDs, only about half of them (126) were selected for analysis, while the other half (124) were eliminated (culled). The selection procedure consisted of culling out neighboring stations from the same cruise that had a correlation of .5 or greater with a selected station. In this way, the average station spacing is about 25 km and the profiles so selected have a greater degree of independence than would otherwise be the case.

Month/Year	Number of Selected	CTD Stations Culled	Total
April 1988	7	5	12
August 1988	5	10	15
September 1988	7	5	12
November 1988	11	2	13
February 1989	9	3	12
March 1989	7	6	13
May 1989	7	4	11
July 1989	5	6	11
September 1989	5	9	14
November 1989	8	7	15
January 1990	5	9	14
March 1990	6	7	13
May 1990	7	8	15
June 1990	5	10	15
August 1990	5	8	13
October 1990	5	8	13
December 1990	10	4	14
February 1991	6	8	14
April 1991	6	5	11
TOTAL	126	124	250

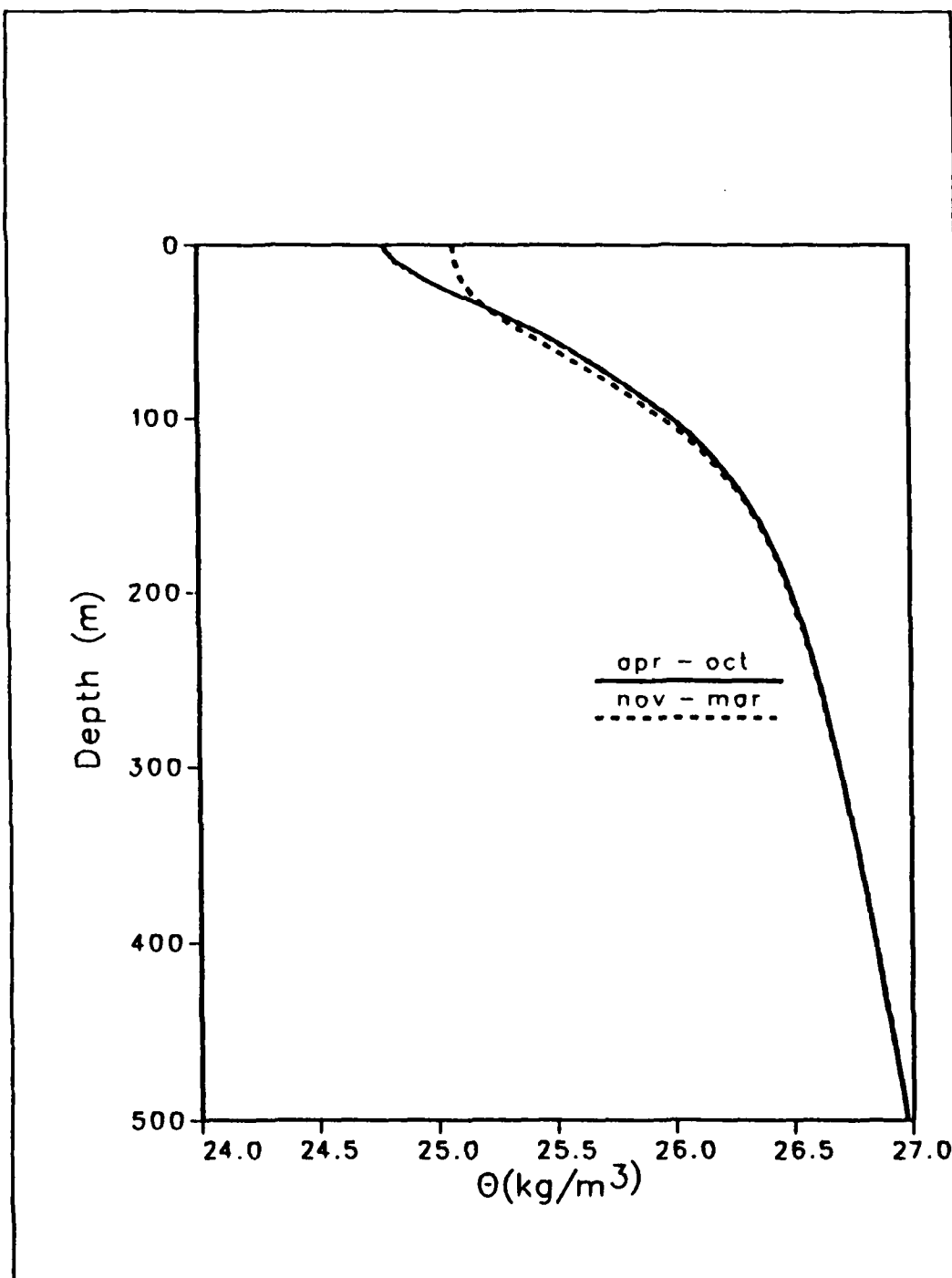


Fig. 2. Mean profiles of density ($\theta - 1000$) to 500 m (a) and buoyancy frequency to 2000 m (b). For Apr - Oct the sample size is 64 and for Nov - Mar it is 62 (see Table 1).

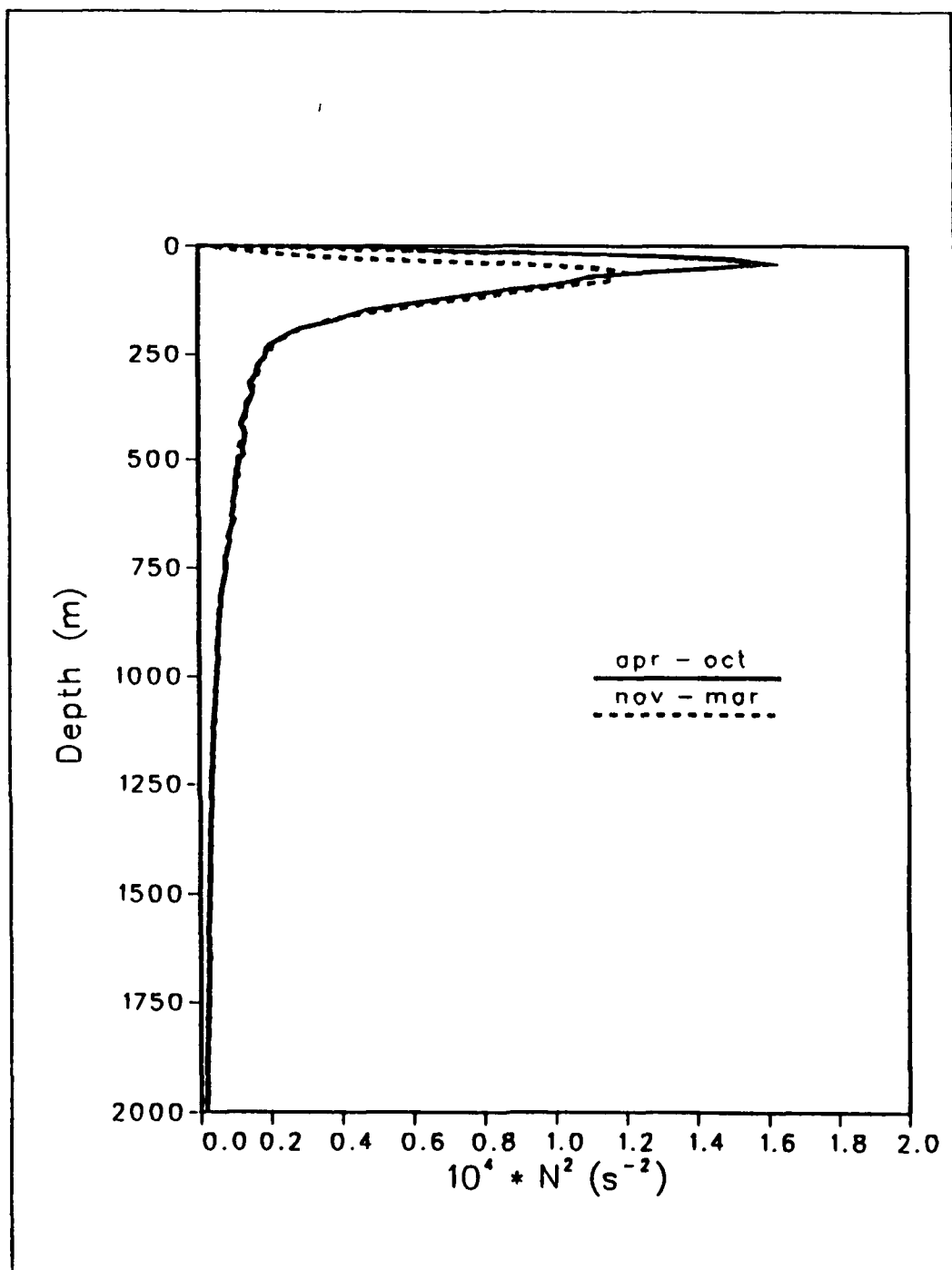


Fig. 2b.

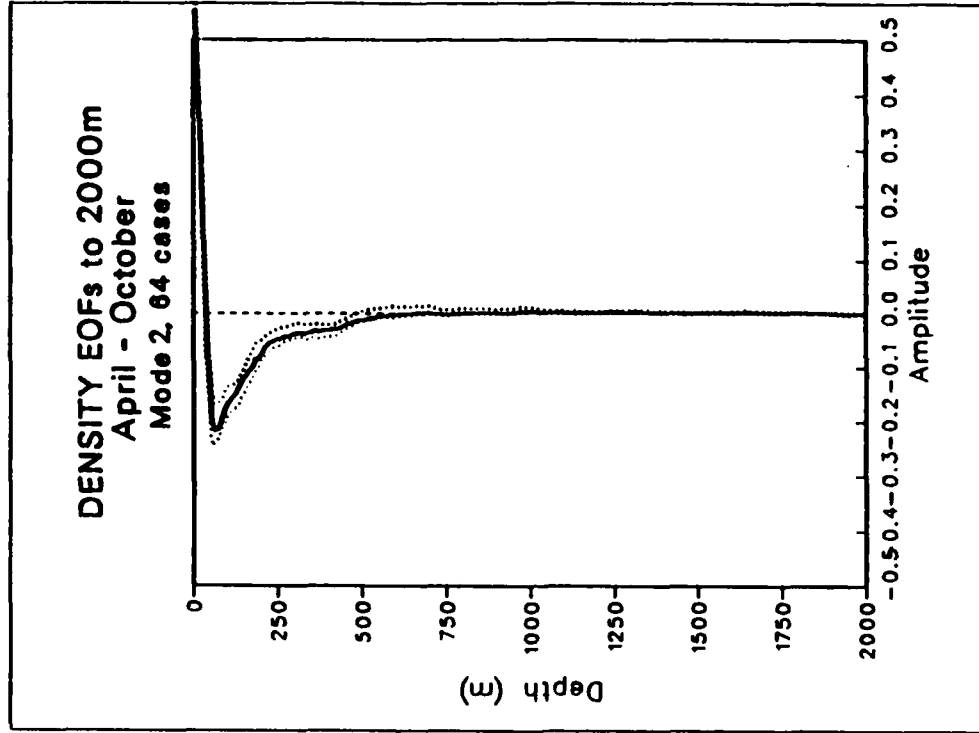
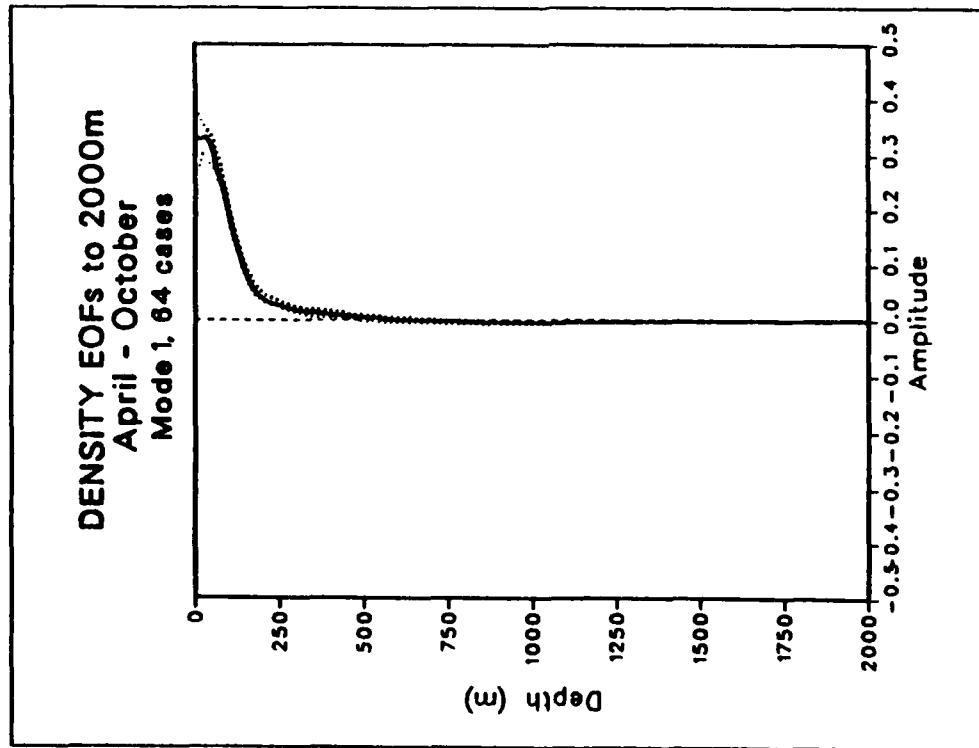


Fig. 3. Density EOFs (kg m^{-3}). (a) Apr - Oct, 64 stations. The 95% confidence limits are estimated using the bootstrap method described in the text.

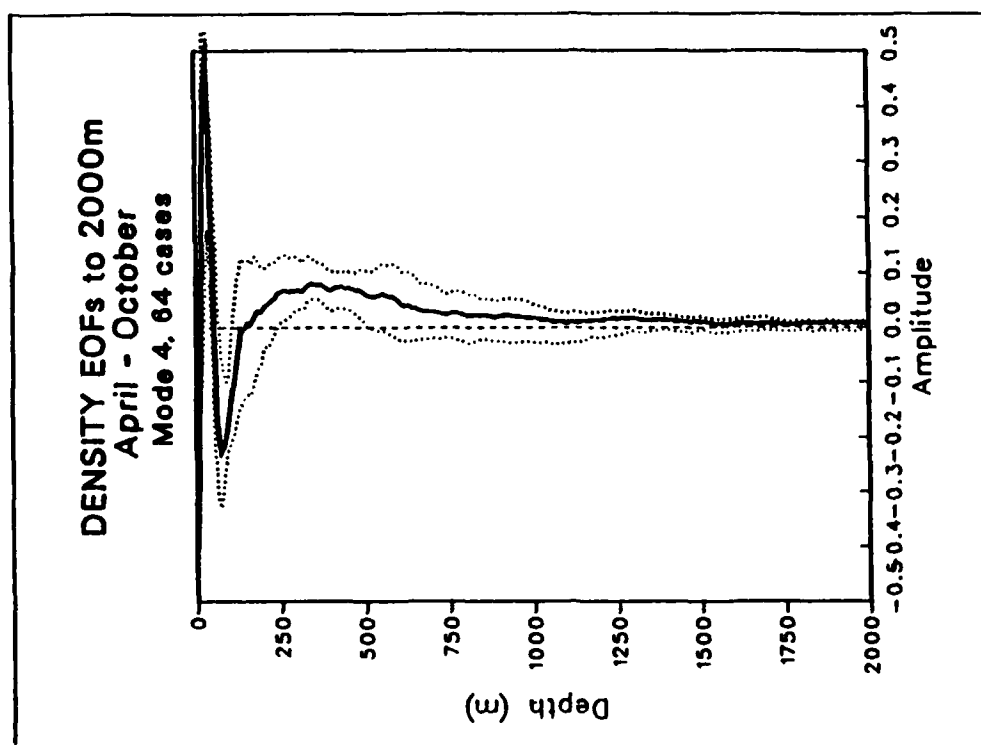
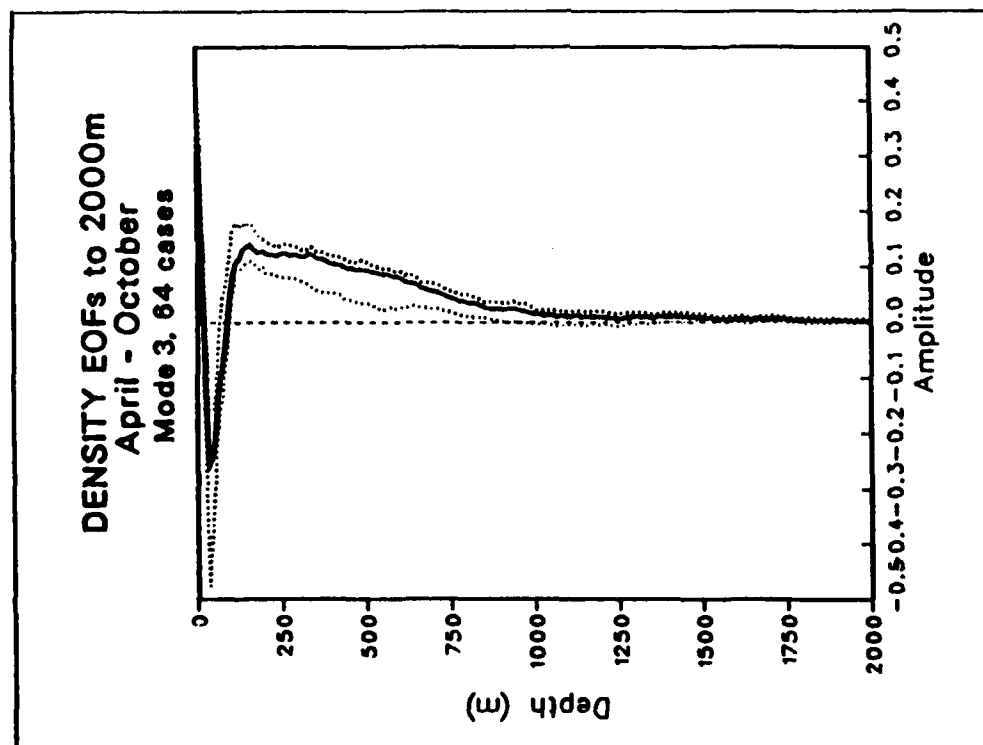


Fig. 3a (continued).

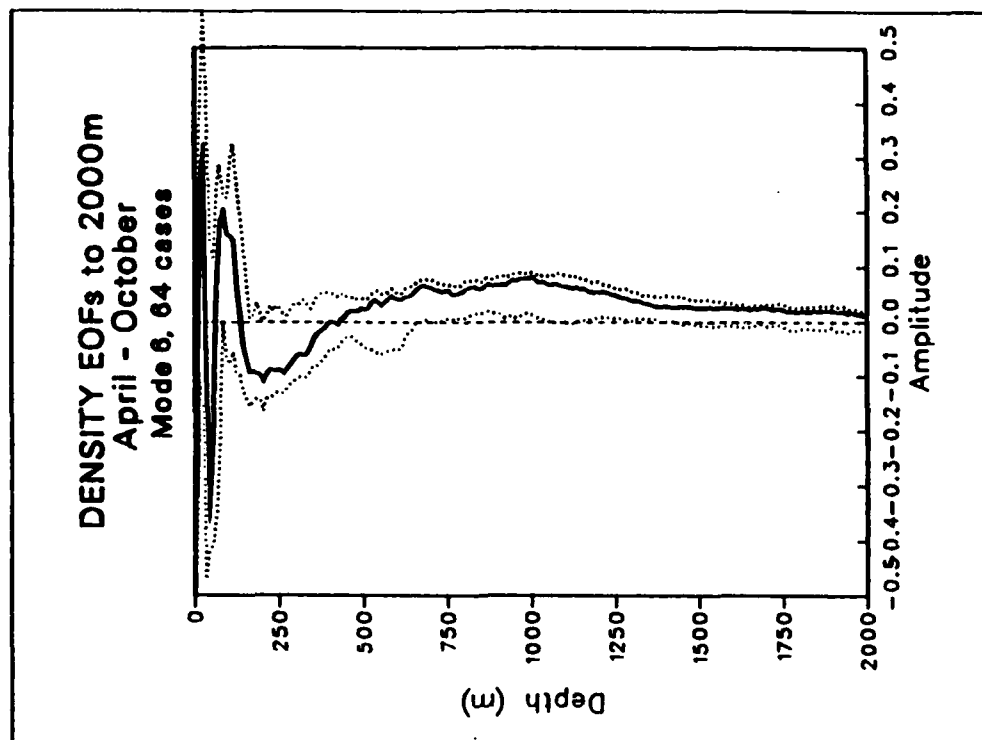
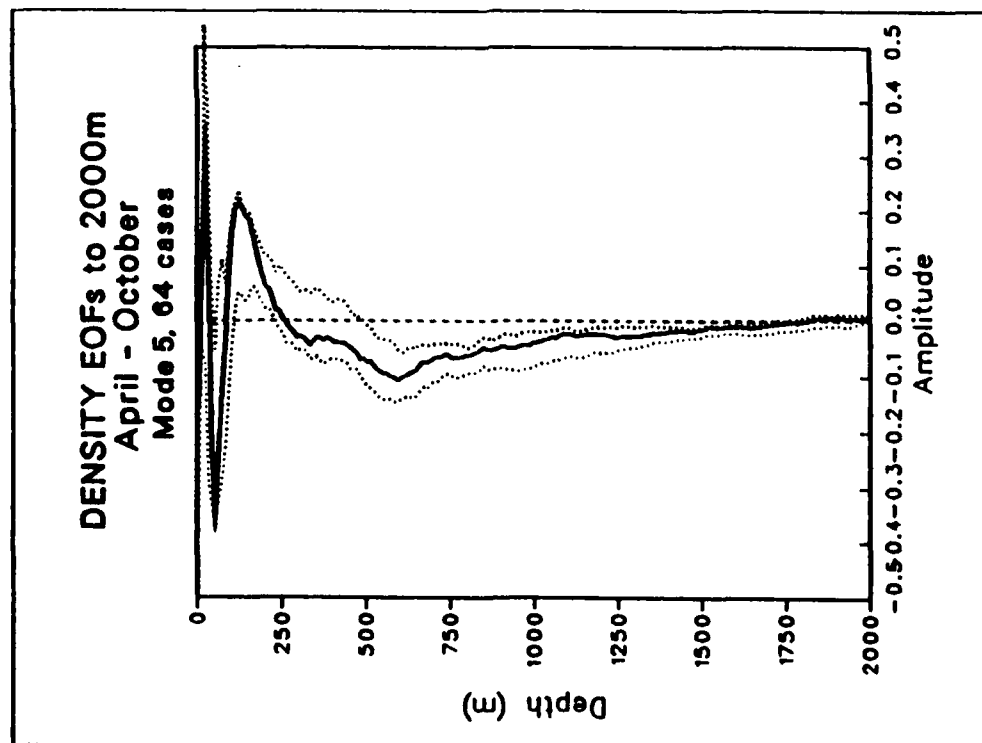


Fig. 3a. (continued).

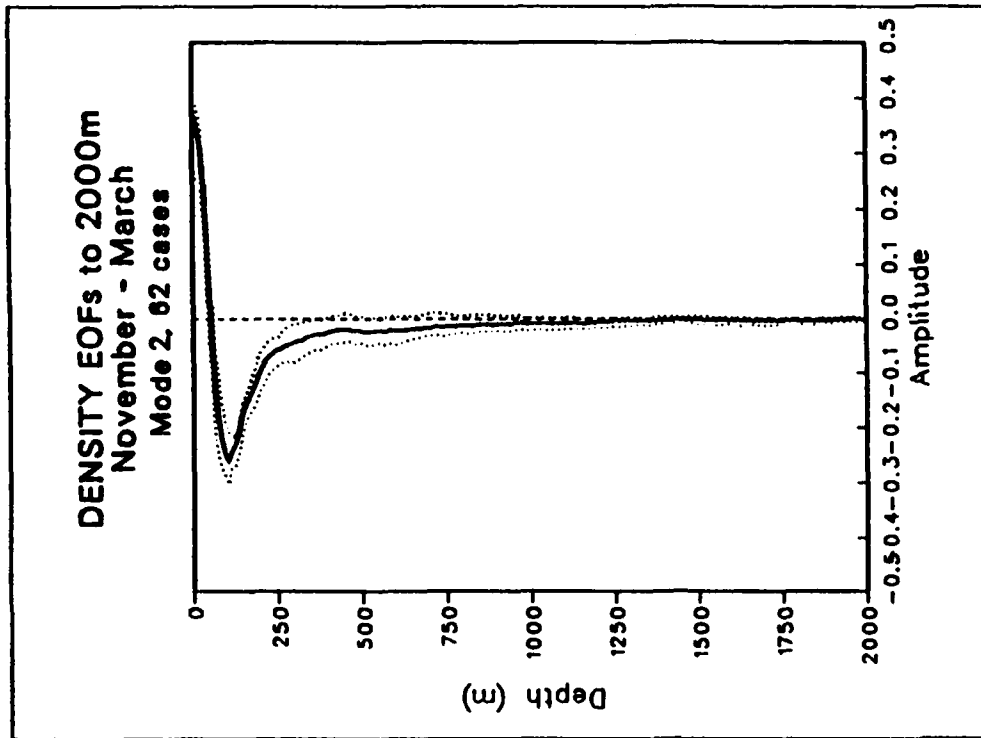
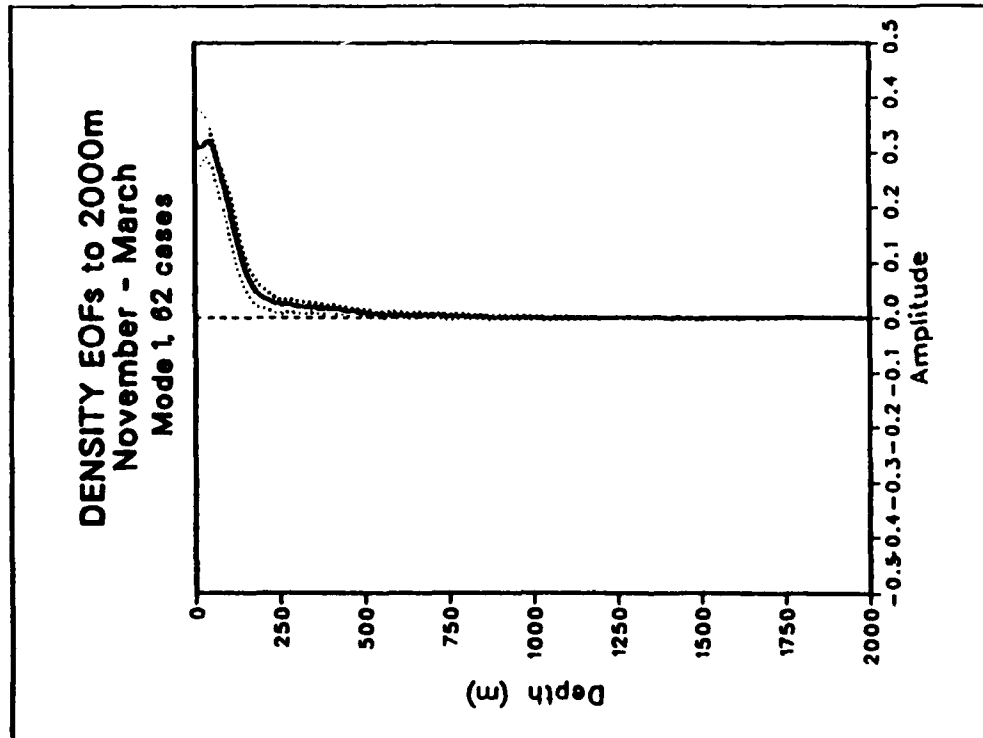


Fig. 3. Density EOFs (kg m^{-3}). (b) Nov - Mar, 62 stations. The 95% confidence limits are estimated using the bootstrap method described in the text.

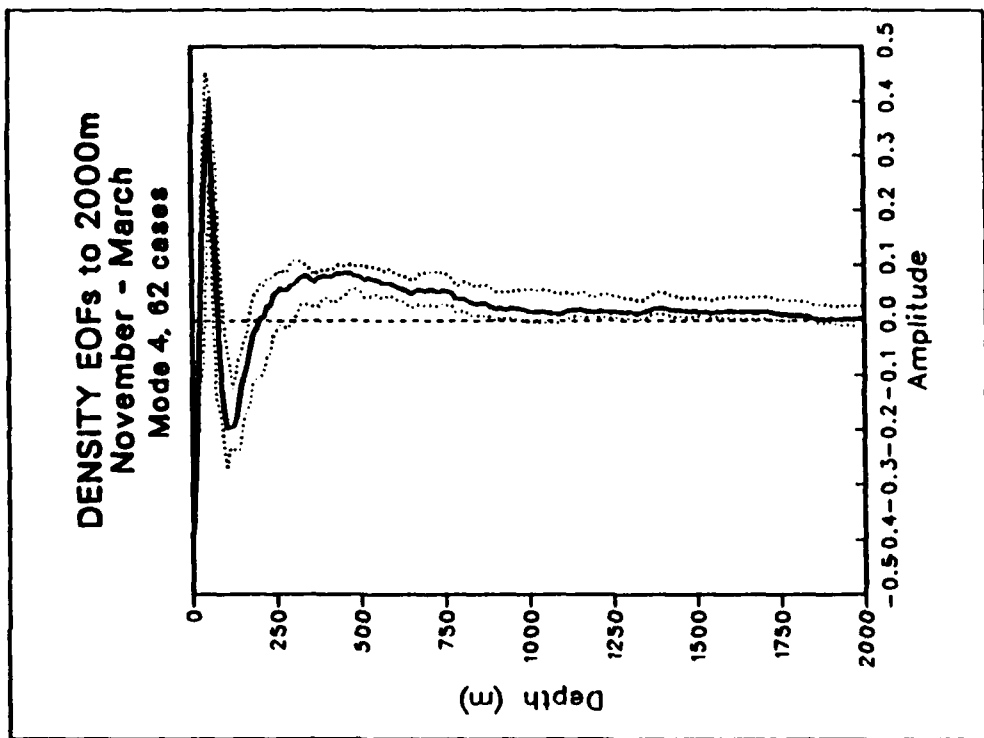
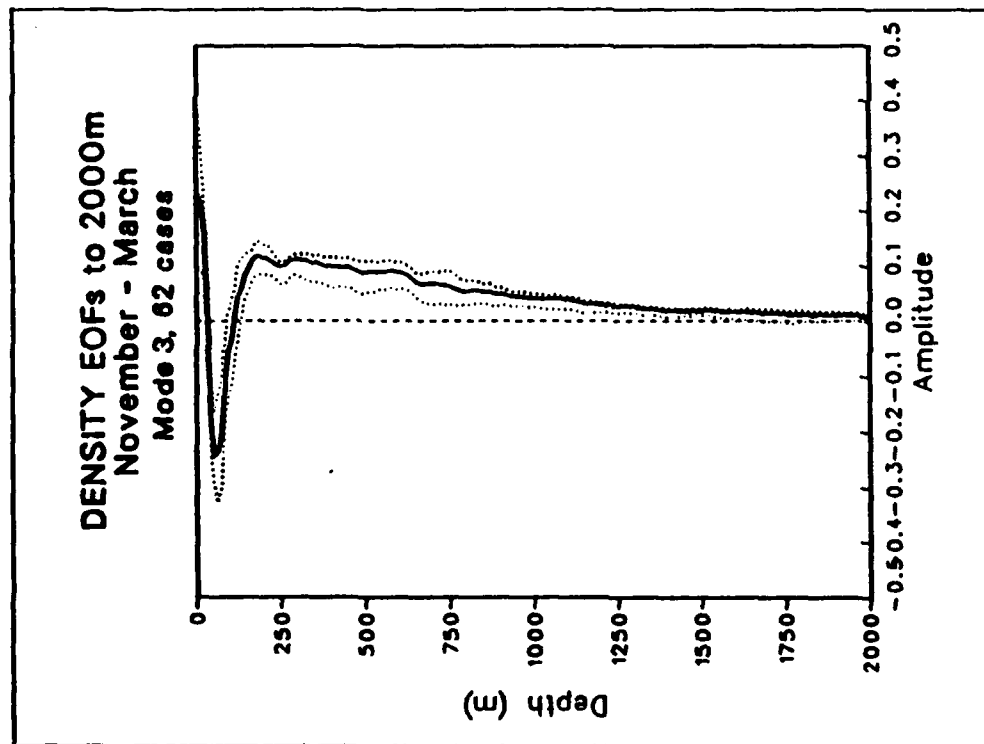


Fig. 3b. (continued)

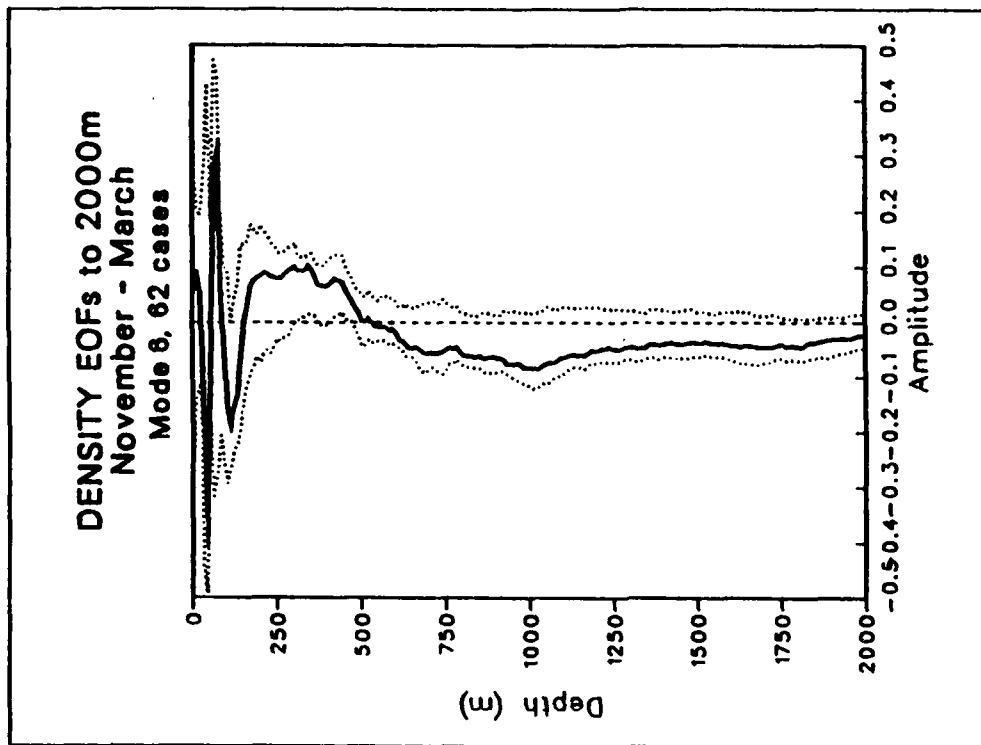
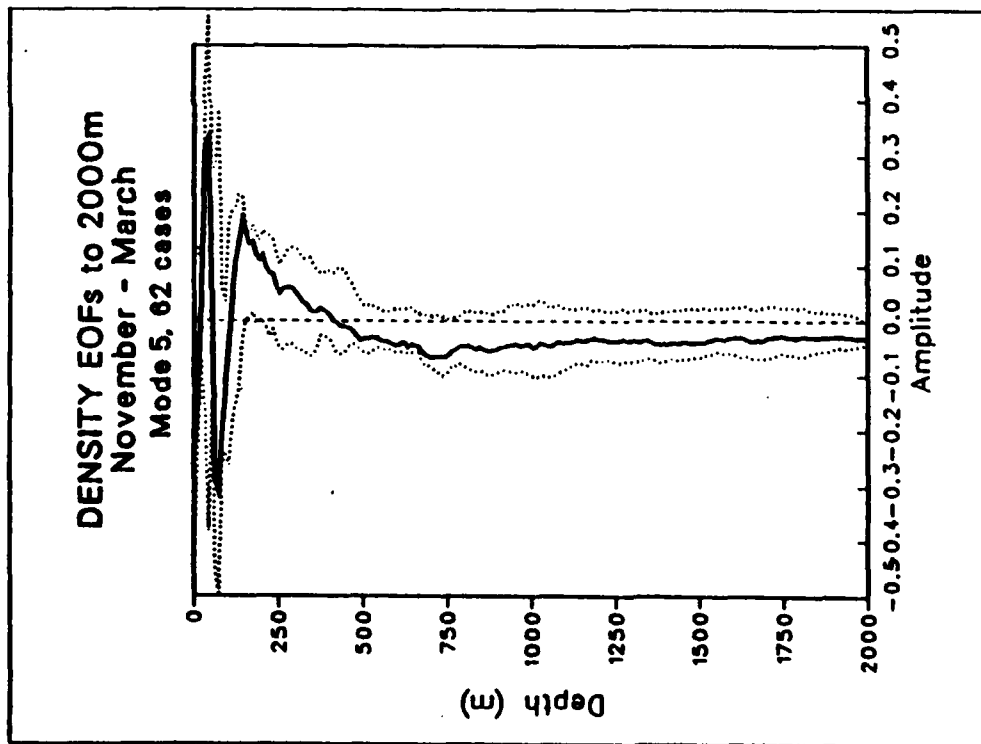


Fig. 3b. (continued)

interpretation is that if a group of true eigenvalues lies within one or two $\delta \lambda$ of each other (i.e., if $\Delta \lambda \leq \delta \lambda$) then they form an "effectively degenerate multiplet", and the sample eigenvectors (EOFs) are simply a random (non-unique) mixture of the true eigenvectors (North *et al.* 1982). Table 2 shows the results of the eigenvalue test. The shapes of no more than the first 5 EOFs in summer and the first 4 EOFs in winter appear to be significant, with overlapping degenerate pairs occurring among higher order EOFs. However fewer EOFs may in fact be significant since North *et al.*'s criteria uses a relatively low level of significance and our data are not entirely independent. In the bootstrap method, a random number generator is used to draw a resample of ND new density profiles, with replacement, from the original ND profiles (this resample may have more than one copy of some profiles, and none of others) and an EOF analysis of this resample is performed. This procedure is repeated many times and the distribution of the results is used to specify the confidence limits shown in Fig. 3. The 95% confidence limits on the shapes of the EOFs shown in Fig. 3 also indicates that the first 5 EOFs in summer and the first 4 EOFs in winter are significant, i.e., have tight confidence limits away from zero.

Although as many as 4 or 5 EOFs may be robust in the sense discussed above, we will only attempt to ascribe a physical meaning to the first two modes. In general, the density EOFs in Fig. 3 are similar to those presented in previous studies of this region (Chelton 1980; Smith *et al.* 1985; Rienecker *et al.* 1987). Comparing Figs. 3a and 3b, it can be seen that there is very little seasonal difference apart from a slight vertical displacement of the modes in summer compared to winter. The first mode represents variability associated with the equatorward vertical shear of the California Current in the main

Table 2. First 12 eigenvalues and their estimated standard error using the method of North *et al.* 1982 described in the text. The standard error $\delta \lambda \sim \lambda e$, where $e = (\frac{2}{N})^{1/2}$ and N is the number of profiles used (64 in summer and 62 in winter).

Mode #	$\lambda - \delta \lambda$	λ	$\lambda + \delta \lambda$	$\lambda - \delta \lambda$	λ	$\lambda + \delta \lambda$
1	1.0672	1.2963	1.5255	0.6131	0.7473	0.8815
2	0.1734	0.2106	0.2479	0.1482	0.1806	0.2131
3	0.0476	0.0578	0.0680	0.0494	0.0602	0.0710
4	0.0259	0.0315	0.0370	0.0142	0.0173	0.0204
5	0.0142	0.0172	0.0202	0.0077	0.0094	0.0111
6	0.0079	0.0096	0.0113	0.0064	0.0078	0.0092
7	0.0065	0.0079	0.0093	0.0035	0.0042	0.0050
8	0.0036	0.0044	0.0051	0.0031	0.0038	0.0045
9	0.0021	0.0025	0.0030	0.0018	0.0022	0.0025
10	0.0016	0.0020	0.0023	0.0015	0.0018	0.0021
11	0.0013	0.0016	0.0019	0.0013	0.0015	0.0018
12	0.0011	0.0013	0.0016	0.0010	0.0012	0.0015

seasonal pycnocline that slopes upward toward the coast in the upper 500 m (Chelton 1980). Note that in the present analysis, in which the CTD stations are from different locations as well as at different times, variability represented by the EOFs can be either spatial or temporal or both. The second mode, which is similar to the first mode except for a change in sign above about 70 m, resembles the second, or "seasonal mode", identified off Northern California by Bray and Greengrove (1993). It is interpreted here as the offshore response of the mixed layer and main pycnocline to local variations in the alongshore wind stress. Seaward of the shelf and slope, upwelling favorable winds, for example, produce offshore transport in the mixed layer and downward motion in the pycnocline below. This leads to density increases in the mixed layer (due to horizontal advection) and density decreases in the pycnocline (due to vertical advection) with a zero crossing near the base of the mixed layer as seen in Fig. 3. Note that mode 1, and also mode 2 in summer, has a significant amplitude only in the upper 500 m. These relatively shallow modes of variability obviously can not be very helpful in estimating density fluctuations below 500 m from observations above that depth. On the other hand, the third and fourth modes, and the second mode in winter, which have significant signals below 500 m, can be useful in this regard if they can be detected in shallow CTD casts.

The above results concerning the statistical significance of the EOF shapes is consistent with the study of North *et al.* (1982). They showed that for many cases of geophysical interest the sampling errors are often unacceptably large for samples of even a few hundred independent realizations. It is important to note, however, that in this study *we are not especially concerned with the shapes of the EOFs per se*. In the present application,

we wish only to have a convenient basis set for representing disturbance density profiles. The sample EOFs computed from our finite data set form such a complete basis set and a subsum of these EOFs is expected to account for about as much variance as the corresponding subsum of the true EOFs (North *et al.* 1982).

Note that the above tests on the EOF shapes provide no guidance in determining the number of EOFs that can represent the profiles efficiently. For this purpose, additional assumptions about the nature of the "noise" in the data must be made. In this study we follow the ideas of Preisendorfer *et al.* (1981) and Smith *et al.* (1985). To distinguish signal from noise, Preisendorfer *et al.* (1981) compare the computed eigenvalues, or (equivalently) the percent of explained variance, with the eigenvalues (or the percent of explained variance) generated by simulated density data having the same variance profiles as the original data, but having no correlation with depth (Fig. 4). Although there is some subjectivity in applying this method, the results in Fig. 4 suggest that only the first two EOFs can be attributed to a vertically coherent signal. As pointed out by Smith *et al.* (1985), this test does not allow each successive eigenvalue to be evaluated independently of the lower modes. To allow for this, and to compare each successive eigenvalue equally, Smith *et al.* (1985) compare the percent of residual variance explained by a given mode to the corresponding value generated by the simulated data. In this way, the variance explained by the first EOF does not affect the evaluation of the second EOF, and the variance explained by the second EOF does not affect the evaluation of the third EOF, etc. The result of this calculation (Fig. 5), taking into account the uncertainty of the eigenvalues (bootstrapped confidence limits), indicates that the first seven EOFs contain a vertically

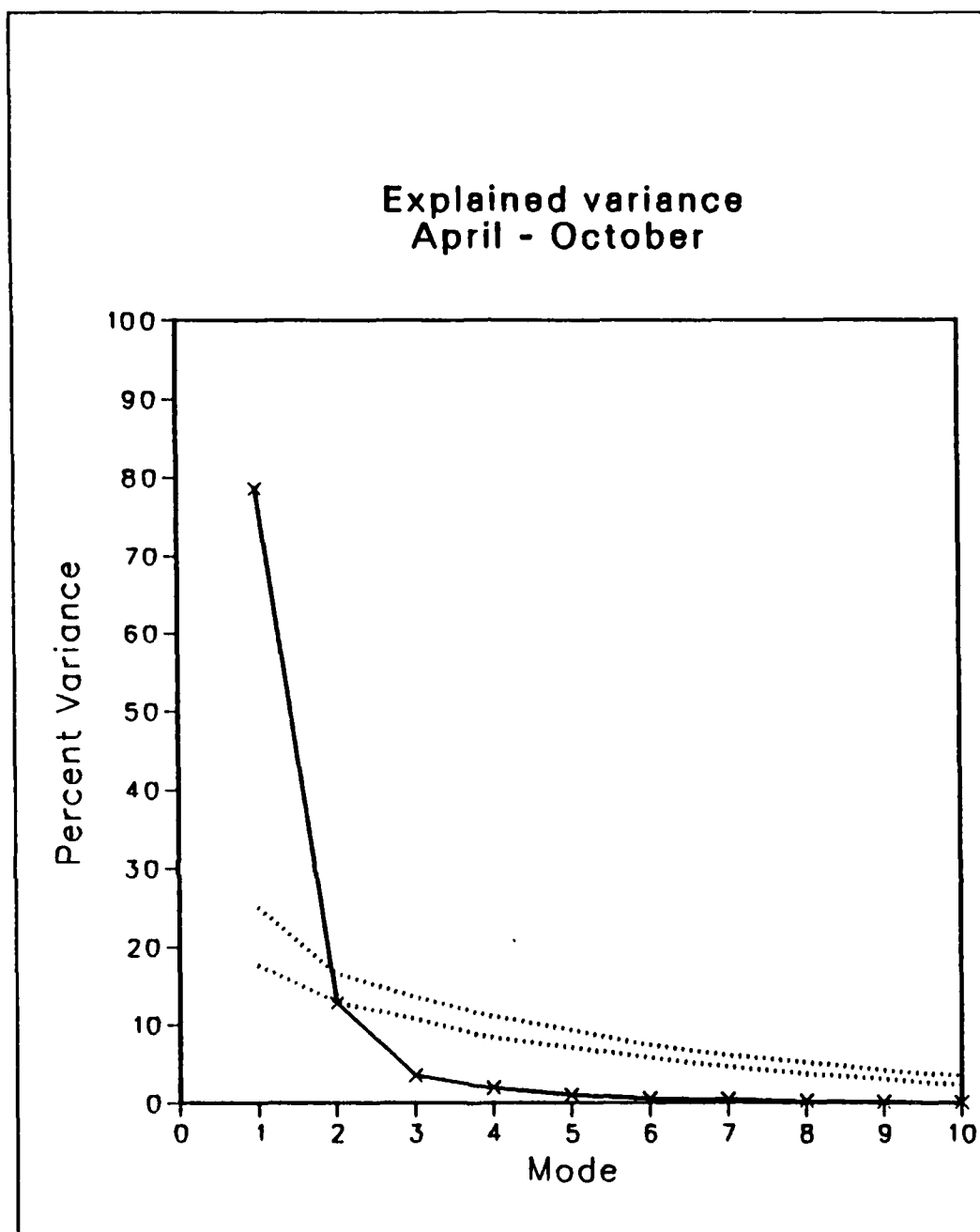


Fig. 4. Percent of variance (scaled eigenvalue) accounted for by each EOF, up to mode number 10, for both the actual (screened) data (top curves) and the simulated data (bottom curves). (a) Apr - Oct and (b) Nov - Mar. The 95% confidence limits on the simulated data are estimated using the bootstrap method described in the text.

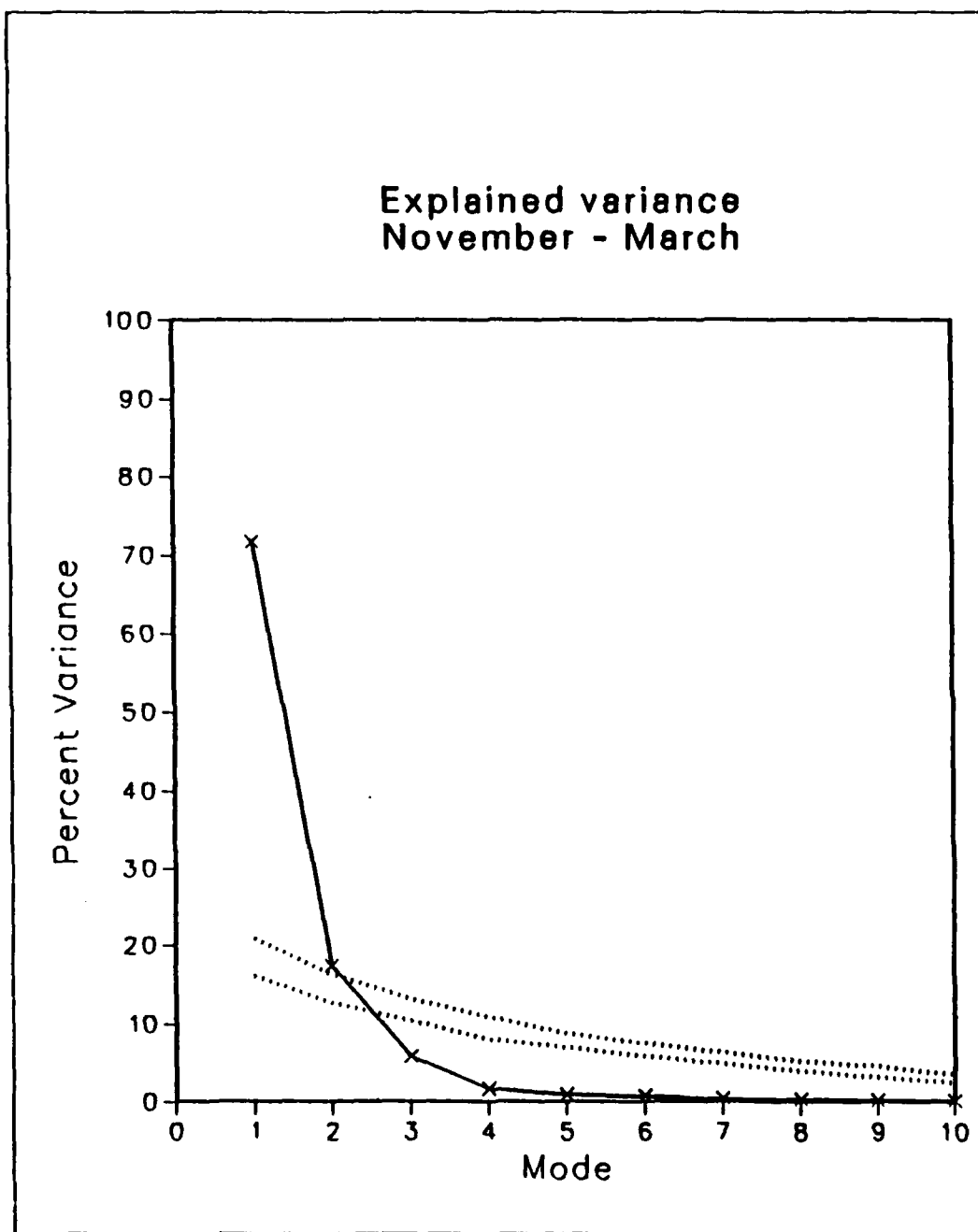


Fig. 4b.

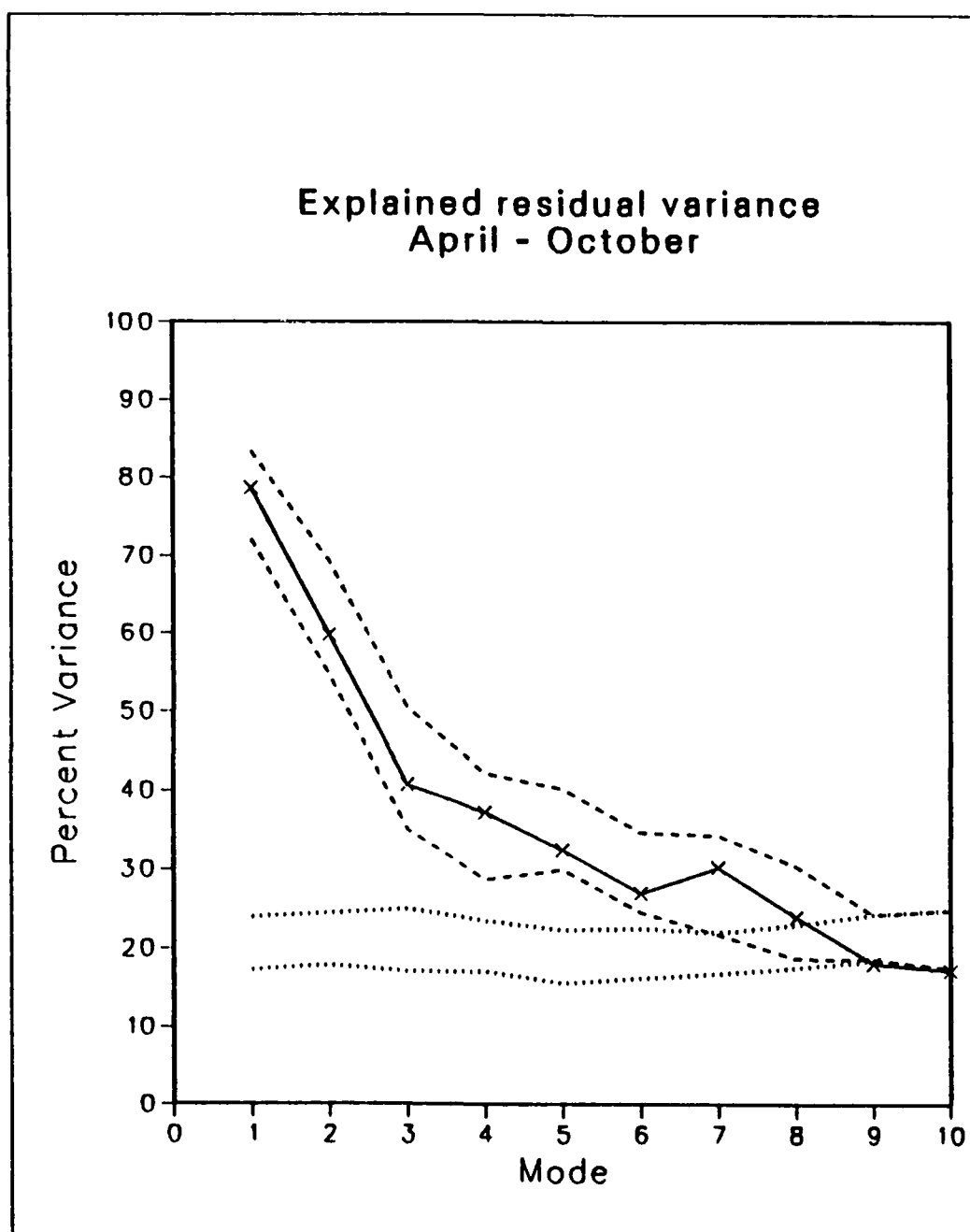


Fig. 5. (a) Same as Fig. 4, except the percent of residual variance accounted for by each EOF is shown.

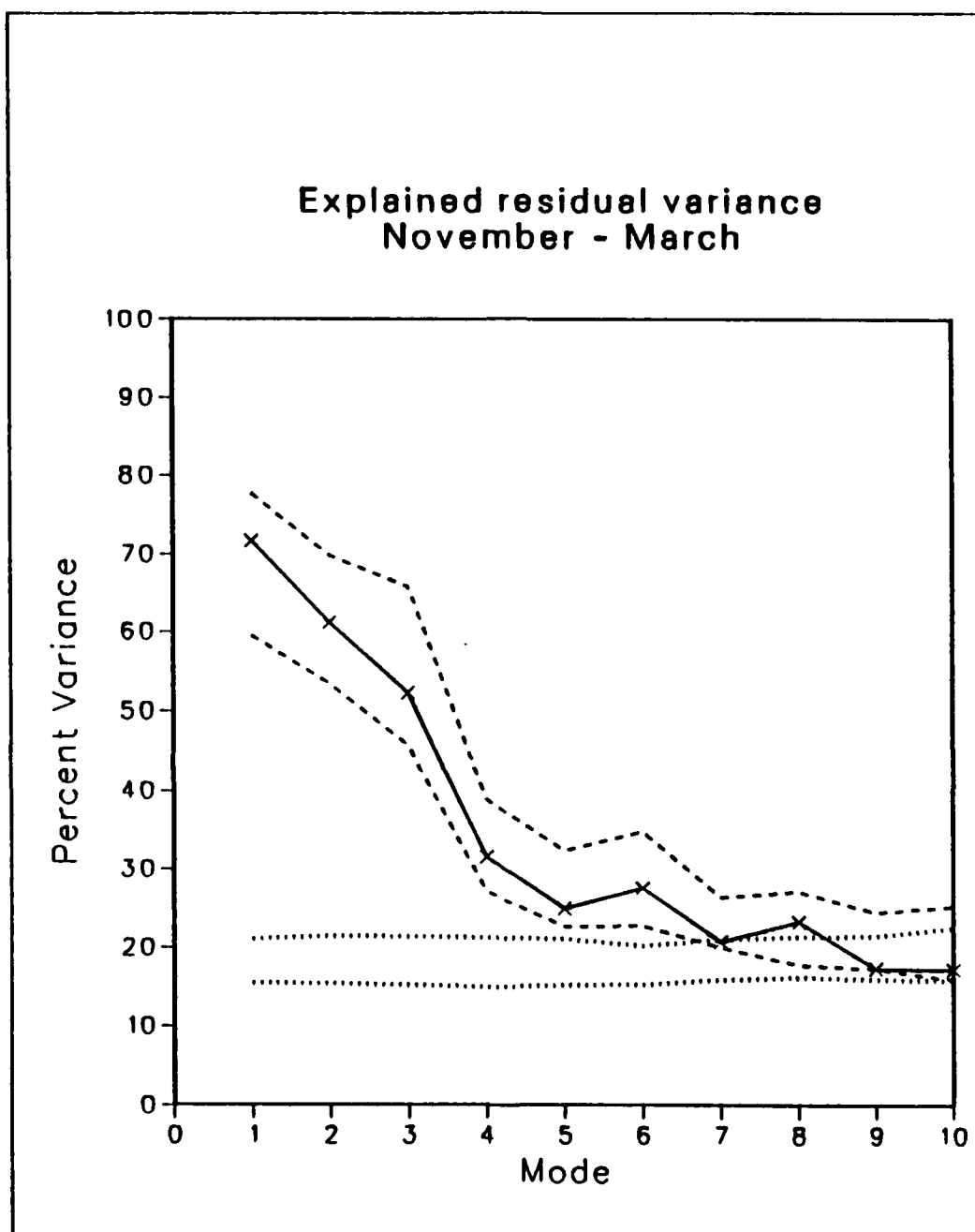


Fig. 5 (b). Same as Fig. 4, except the percent of residual variance accounted for by each EOF is shown.

coherent signal. The result of this test is therefore quite different from that of the Preisendorfer *et al.* (1981) test (Fig. 4). A subjective comparison between the observed profiles of disturbance density and the corresponding profiles reconstructed from the first seven EOFs (see Fig. 11, first frames) supports the choice of seven modes for the cut-off between signal and noise. At the same time, a similar comparison between the observed profiles and those reconstructed from only 2 modes (not shown) reveals large differences that most physical oceanographers would not consider attributable simply to "noise". On the basis of this analysis, subjective as it admittedly seems to be, we consider all of the profile variability that is contained in the first seven modes to be "signal" and the remaining variability to be "noise". In total, the first seven modes account for over 99 percent of the variance in both winter and summer (Table 2). Having identified the first 7 EOFs as a convenient basis set for describing the observed "signal", we now examine the extent to which these modes can be identified from shallow CTD casts (to $Z = D < 2000\text{ m}$) and used to estimate the profiles below D.

4. Results of Vertical Extension

In this section, density profiles below the depth D are estimated by fitting the first 7 EOFs to the selected profiles above D. The accuracy with which an estimated profile (E) matches an observed profile (O) is measured by their correlation coefficient, r ,

$$r = \frac{\langle E' O' \rangle}{(\langle E'^2 \rangle \langle O'^2 \rangle)^{1/2}}, \quad (4.1)$$

and a skill score, s ,

$$s = 1 - \frac{\langle (E - O)^2 \rangle}{\langle (O')^2 \rangle} . \quad (4.2)$$

In (4.1) and (4.2), $\langle \rangle$ denotes an average, at a fixed depth, over all of the selected profiles for the half-year in question and $()'$ denotes the departure from this average. Although r and s are both equal to 1 for a perfect estimate, and both decrease as E departs from O , s becomes negative when the mean square error exceeds the observed variance.

Fig. 6 shows how the estimated profiles approach the observed profiles as more and more modes are used, and the fitting is performed over the full water column ($D = 2000$ m). In both halves of the year the correlation and skill are seen to increase as the number of EOF modes that are used to estimate the profiles is increased. The correlation and skill tend to be greater in the upper part of the water column, and to decrease systematically with depth. This is because the successive EOFs are constructed so as to explain the maximum amount of vertically coherent, residual variance, and this is much larger in the upper ocean than at depth. From the earlier discussion about profile "noise", it is clear that the relatively poor correlations below about 1500 m when 7 EOFs are used in the fit (last frame) are entirely due to noise representing no more than 1% of the total variance (Table 3). As the number of EOFs that are used is increased beyond 7 (not shown), the remaining variance is accounted for and r and s approach 1 at all depths. It is interesting that the way in which the individual modes contribute to the total solution is different in summer than in winter. For example, the 2nd and 3rd EOF make important contributions to the correlations at all depths in winter. However in summer, the 2nd EOF seems to be important only in the

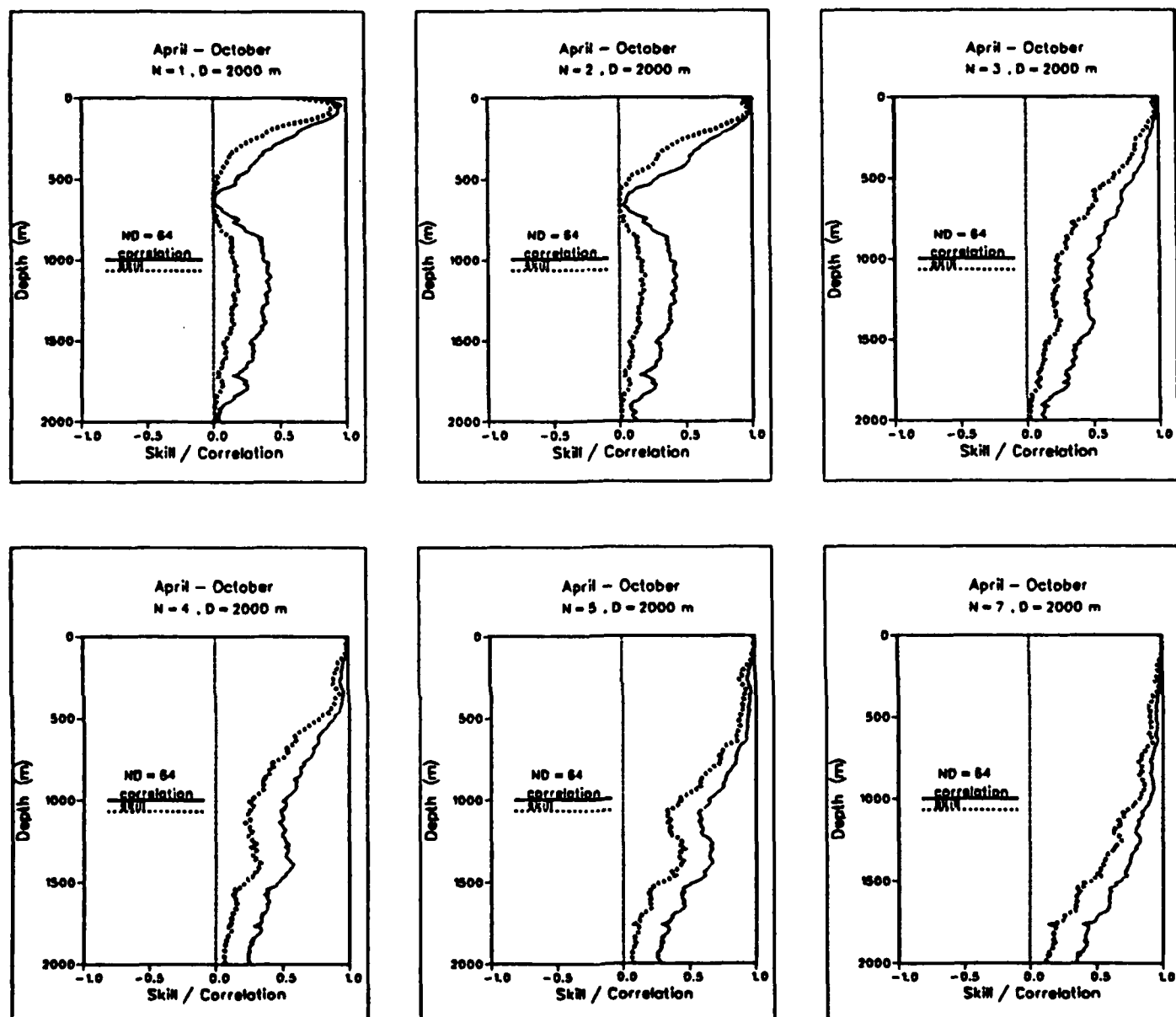


Fig. 6 (a). Correlation (r) and skill (s) of estimating the observed profiles when the fitting is performed to 2000 m, and N EOFs are used. Profiles of r and s are shown for $N = 1, 2, 3, 4, 5$, and 7 for both the summer half-year, Apr - Oct (a) and the winter half-year, Nov - Mar (b). ND is the number of profiles used.

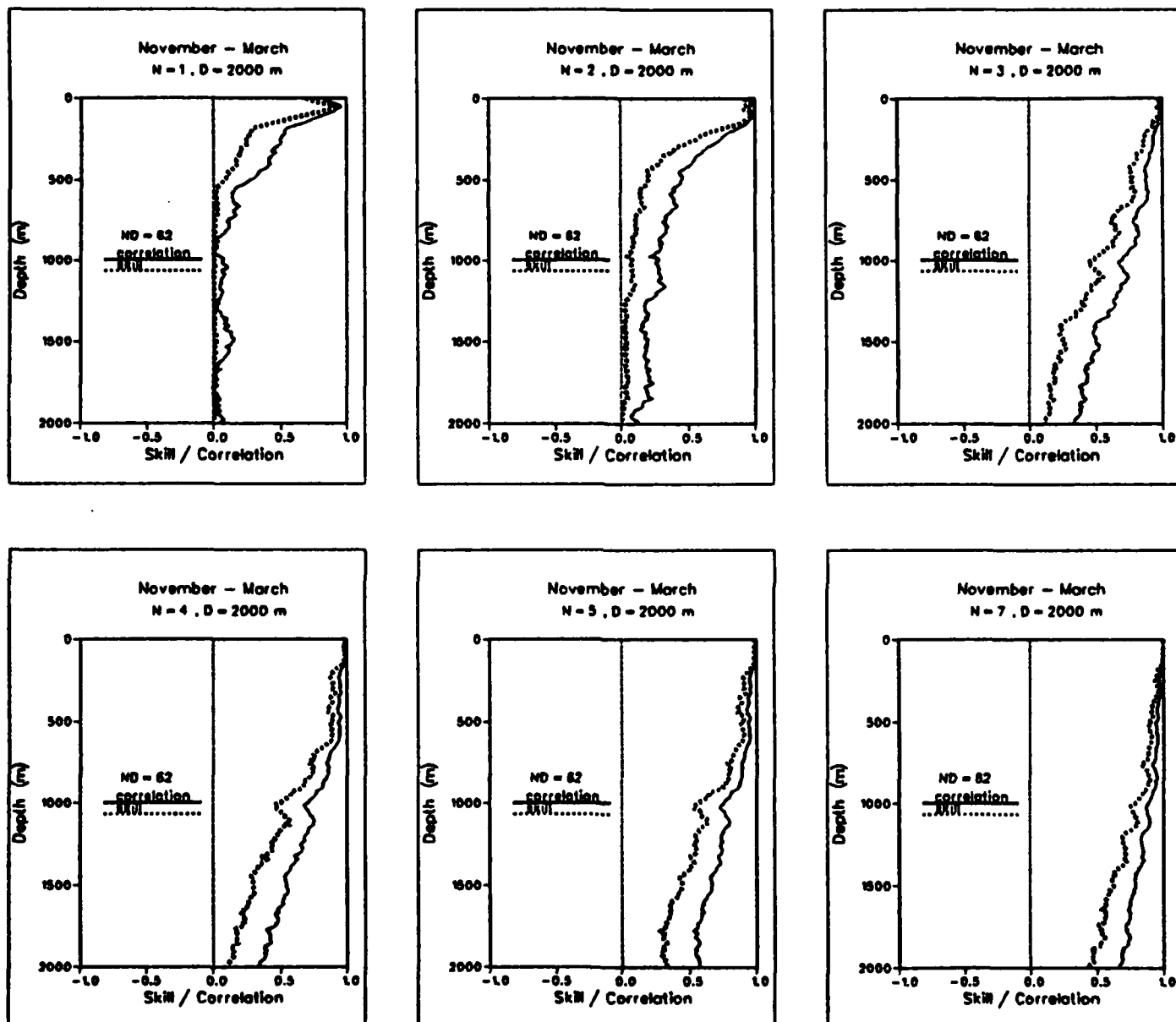


Fig. 6(b).

Table 3. Percent variance (PV) and cumulative percent variance (CPV) accounted for by the first 7 EOF modes. Data taken from Fig. 4.

Mode #	April – October		November – March	
	PV	CPV	PV	CPV
1	78	78	71	71
2	13	91	18	89
3	4	95	6	95
4	2	97	2	97
5	1	98	1	98
6	1	99	1	99
7	< 1	99	< 1	99

mixed layer while the 3rd EOF is very significant in the depth range of 300 - 1000 m.

The central result of this study, the skill of estimating density profiles from data in the upper ocean alone, is presented in Fig. 7. For convenience, we show the results in six separate frames, each frame corresponding to a different value of the depth D used to define the "upper ocean". The successive frames show how well the estimated profiles match the observed profiles, as measured by r and s , as the data-EOF fitting is performed over an increasing depth of the upper ocean. In general, the correlation and skill decrease rather rapidly below D . Furthermore, the decrease with depth is more rapid in summer than in winter. Shallow casts to 200 or 300 m have distinctly less skill at estimating density fluctuations in the 500 - 1000 m depth range in summer than in winter. For example, data to only 200 m can be used to estimate the density disturbances at 500 m with a correlation of about .4 in summer and .6 in winter. This result is operationally significant because shallow casts to 200 m are typical of the SEASOAR CTD system. The drop-off in estimation skill below D (for $D \leq 500$ m say) is due in part to the relatively shallow nature of the major baroclinic features represented by the first 7 EOFs in this region of the California Current.

We now examine the effect of observational "noise" in the CTD profiles. As a result of the analysis presented above, density fluctuations accounted for by EOF modes higher than 7 are considered indistinguishable from vertically incoherent "noise". Since no vertical extension method can be expected to explain such noise, it is of interest to know how well the present EOF method can estimate simply the "noise-free" part of the density profile, i.e., the "signal". To address this issue, we present in Figs. 8 - 9 the same information as in Figs. 6 - 7, except that here the correlation and skill are computed between the estimated profiles

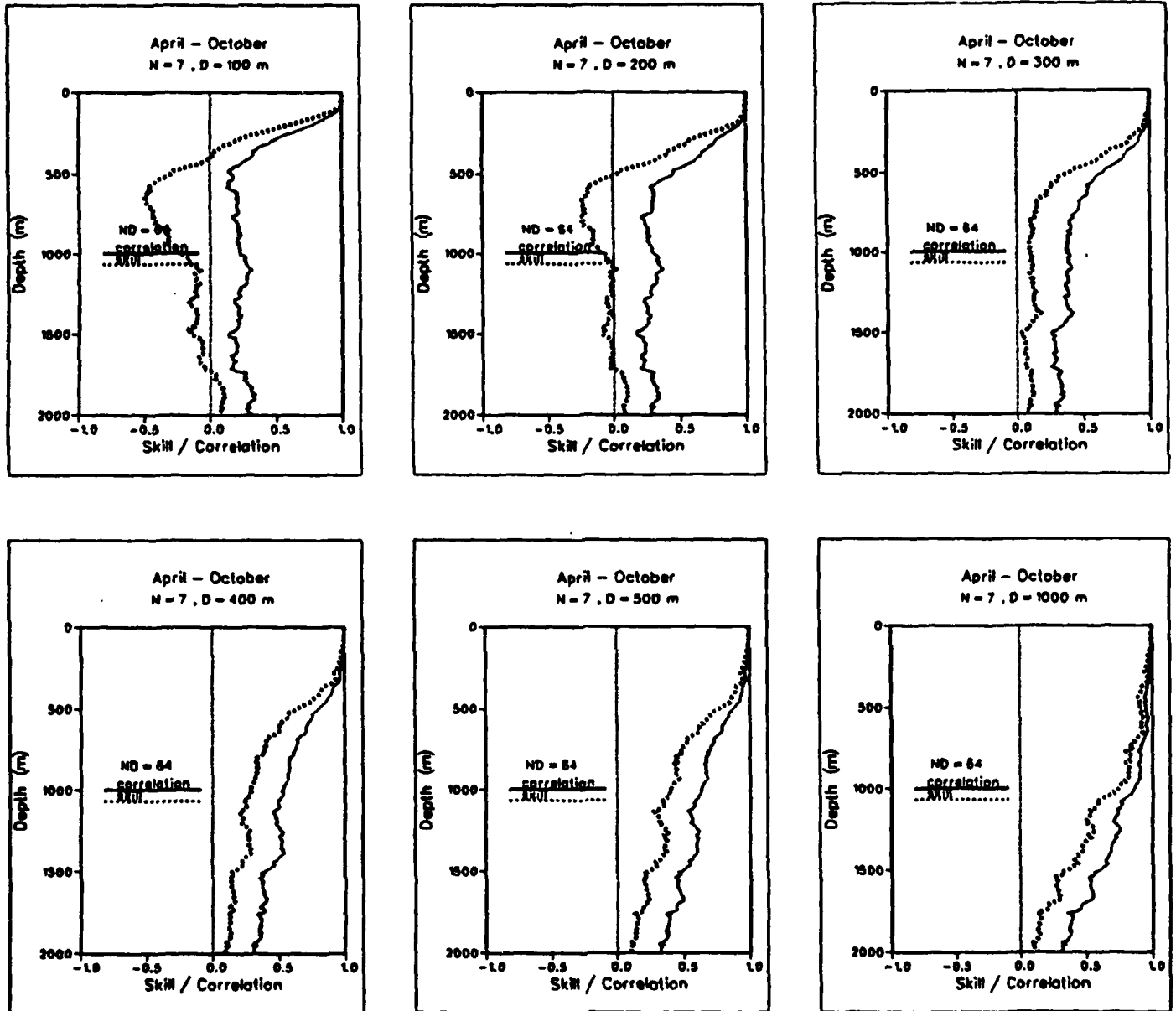


Fig. 7. Correlation (r) and skill (s) of estimating the observed profiles using the first 7 EOFs and data above D , for $D = 100, 200, 300, 400, 500,$ and 1000 m. Profiles of r and s are shown for both the summer half-year (a) and the winter half-year (b).

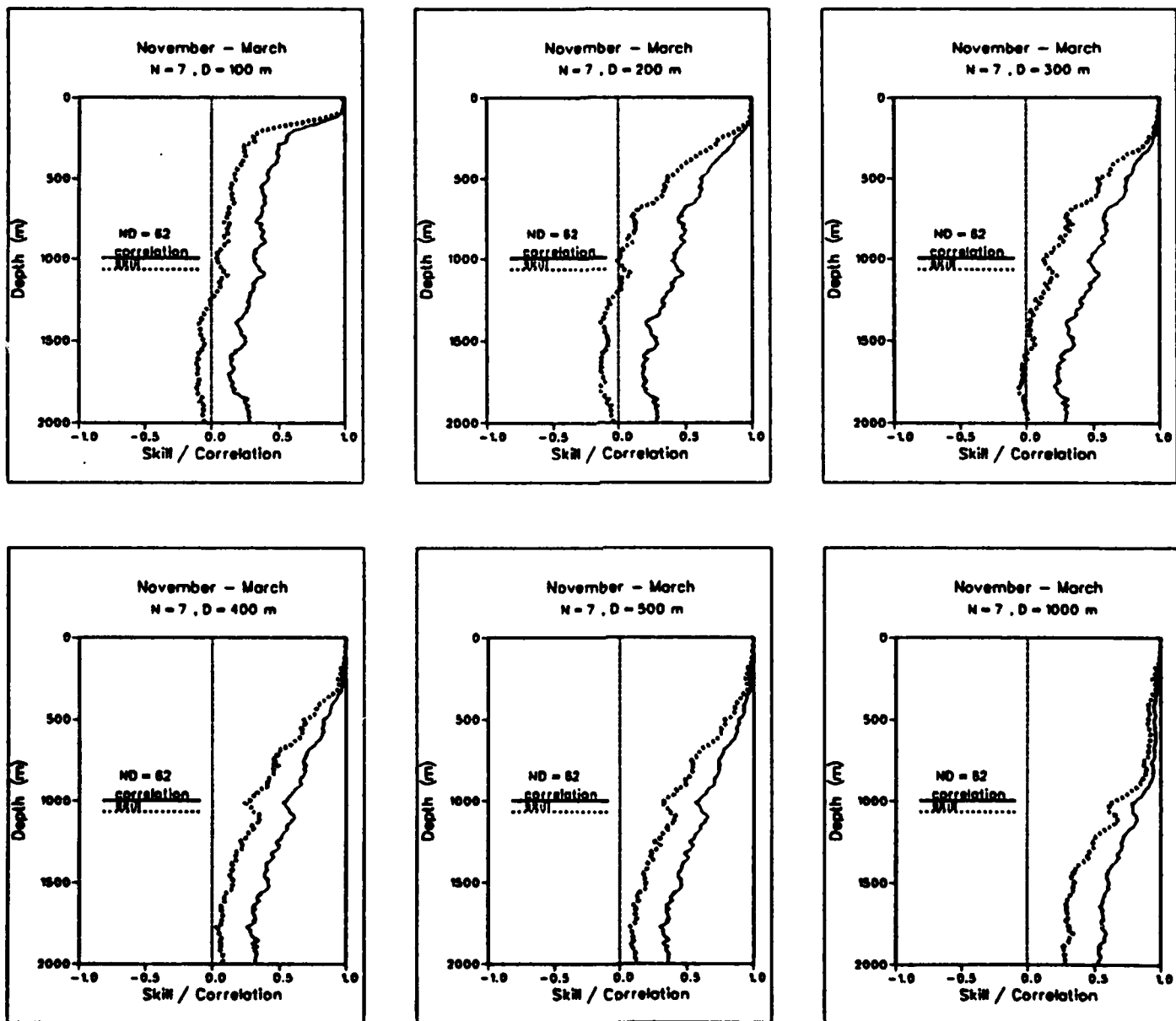


Fig. 7(b)

and the noise-free, or filtered, profiles. The filtered profiles are obtained by fitting the observed profiles (to 2000 m) to the first 7 EOFs. It is not known whether the results shown below are sensitive to this particular method of removing noise from the profiles or whether any other vertical smoothing or filtering operation would produce similar results. Fig. 8 shows how the fit (to 2000 m) to the filtered profiles, as measured by r and s , improves as more modes are used. The fit is nearly exact when 6 modes are used (last frame) since the filtered profiles themselves are reconstructed from only the first 7 modes. The ways in which the various modes contribute to the filtered profiles are different in summer than in winter as seen before in Fig. 6.

The success with which the EOF method can estimate the filtered profiles using data entirely above D , is shown in Fig. 9. This should be compared to the results for estimating the observed, unfiltered, profiles shown in Fig. 7. As with estimating the observed profiles, the correlations and skill also decrease below D , but the decrease is not nearly so rapid for $D \geq 400$ m. In fact, the results show that observations down to only 500 m can be used to estimate the filtered profiles below 500 m quite accurately. For shallower casts, i.e., $D \leq 300$ m, there is also a noticeable improvement compared to estimating the observed, unfiltered, profile but this occurs mostly below 1000 m. The improved correlations in the deeper ocean is entirely due to the removal of noise. The last frame in Fig. 9 shows that the EOF method can estimate the filtered profiles to 2000 m quite accurately with data to only 1000 m.

In an attempt to evaluate the estimation procedure on a somewhat independent set of data, we also applied the method to estimate the culled profiles (Table 1). In this

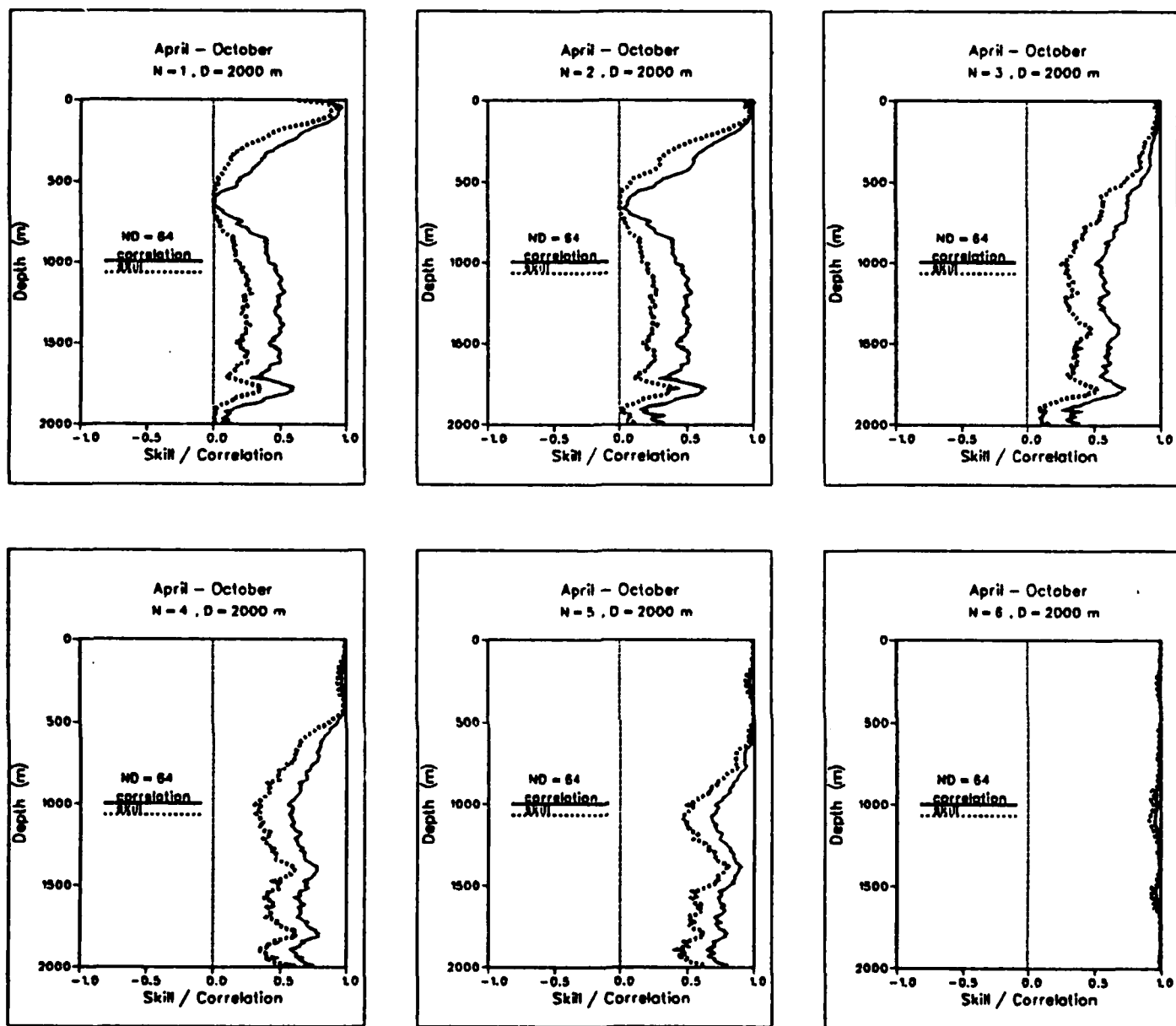


Fig. 8. Correlation (r) and skill (s) of estimating the filtered profiles when the fitting is performed to 2000 m, and N EOFs are used. Profiles of r and s are shown for $N = 1, 2, 3, 4, 5$, and 7 for both the summer half-year, Apr - Oct (a) and the winter half-year, Nov - Mar (b). ND is the number of profiles used.

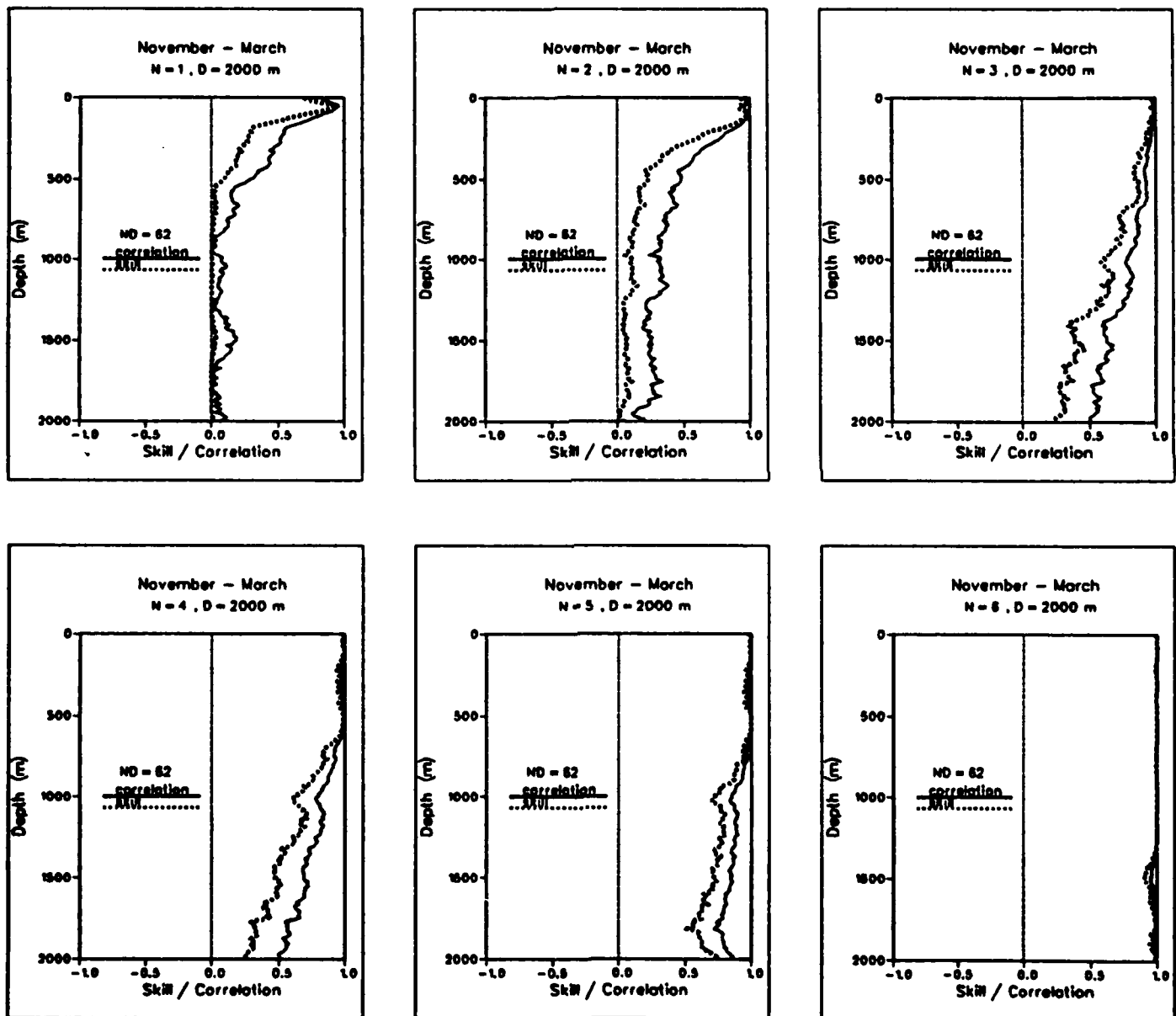


Fig. 8(b).

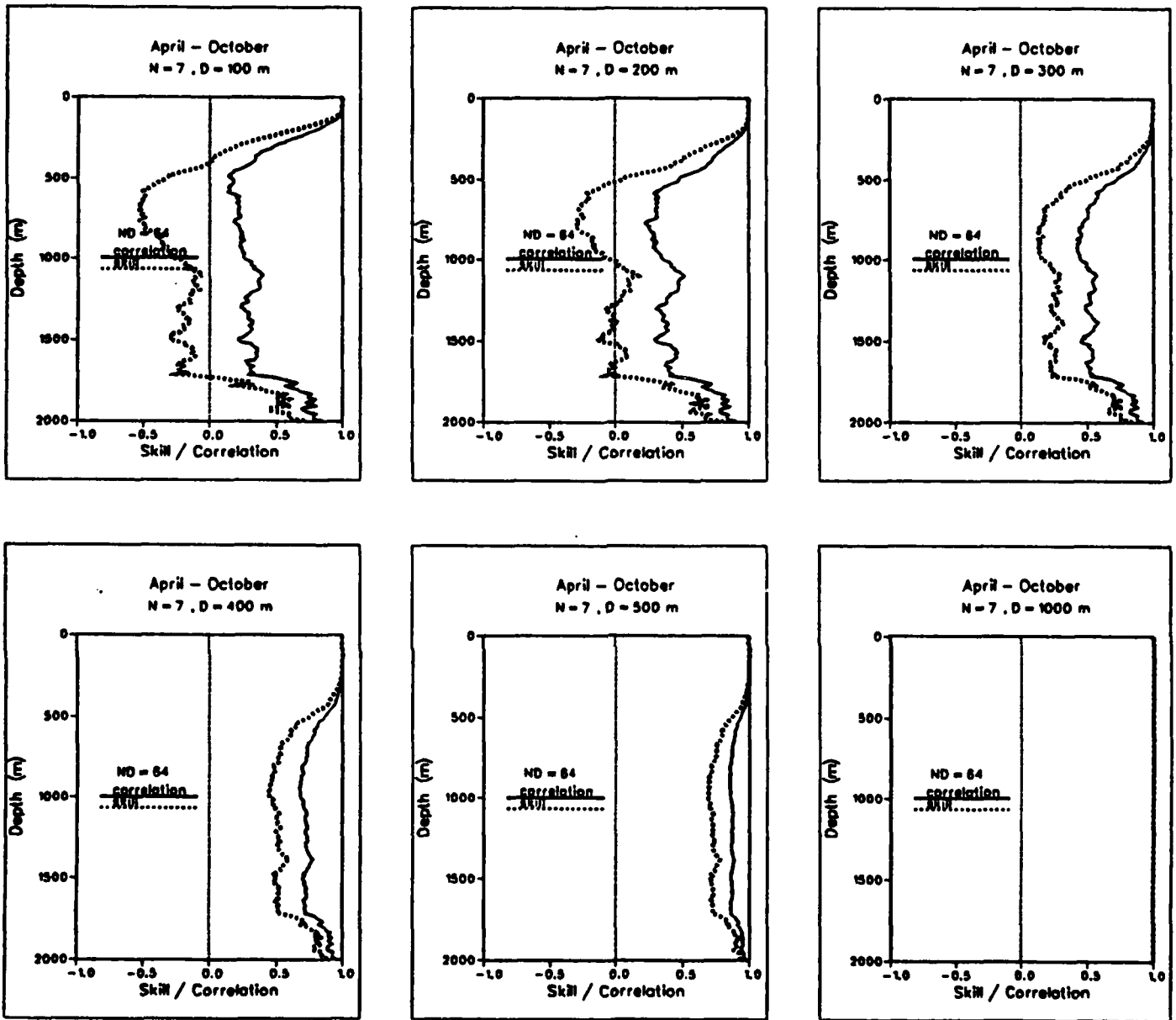


Fig. 9. Correlation (r) and skill (s) of estimating the filtered profiles using the first 7 EOFs and data above D , for $D = 100, 200, 300, 400, 500,$ and 1000 m. Profiles of r and s are shown for both the summer half-year (a) and the winter half-year (b).

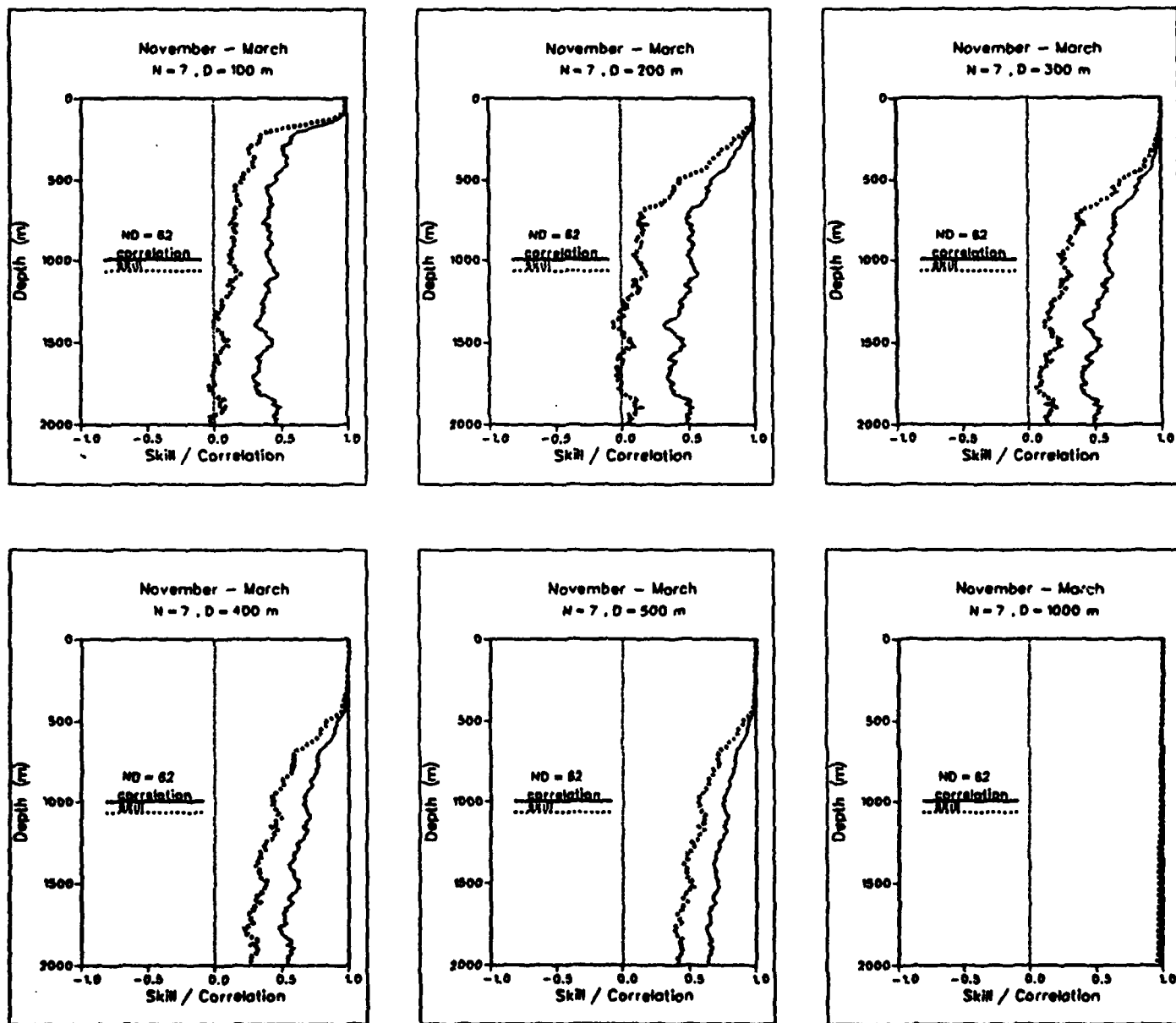


Fig. 9(b).

evaluation, the same seven EOFs that were used to estimate the selected profiles (Fig. 3) were also used to estimate the culled profiles. The results, shown in Fig. 10, are similar to those for the selected profiles (Fig. 9) except that the method is less successful at estimating the culled profiles in winter. This degradation could be due to the smaller sample size used in winter than in summer. Tests with a larger sample of truly independent profiles, ones acquired on different cruises at different times, are needed to determine reliably how well the method would perform in practice.

To compliment the foregoing statistical information on the performance of the EOF estimation method, we present in Fig. 11 a number of direct comparisons between observed and estimated profiles. At least one profile from each of the POST cruises was selected for display in order to show the different performance characteristics of the estimation method. Fig. 11a-t shows the observed and filtered profiles in the top left frame and the estimated profiles, for $D = 200, 300$ and 500 m, respectively, in the other frames.

Some of the features to note in Fig. 11 include the following. The character of the noise in the observed profiles is seen by comparing the observed and filtered profiles in the top left frames. As defined here, "noise" is simply density fluctuations not accounted for by the first 7 EOFs. Some profiles are seen to have very little noise (Fig. 11e, h, and l); some have noise in especially short vertical scales (Fig. 11b, g, r, and t); and other profiles have noise in somewhat larger vertical scales (Fig. 11a, c, m, n, and q). Note that the relatively large amplitude disturbance between $500 - 1500$ m in profile q, which is attributed to noise by comparison with the filtered profile, does not appear at a nearby profile from the same cruise (r), and in fact it does not appear in any other profile from that cruise (not shown).

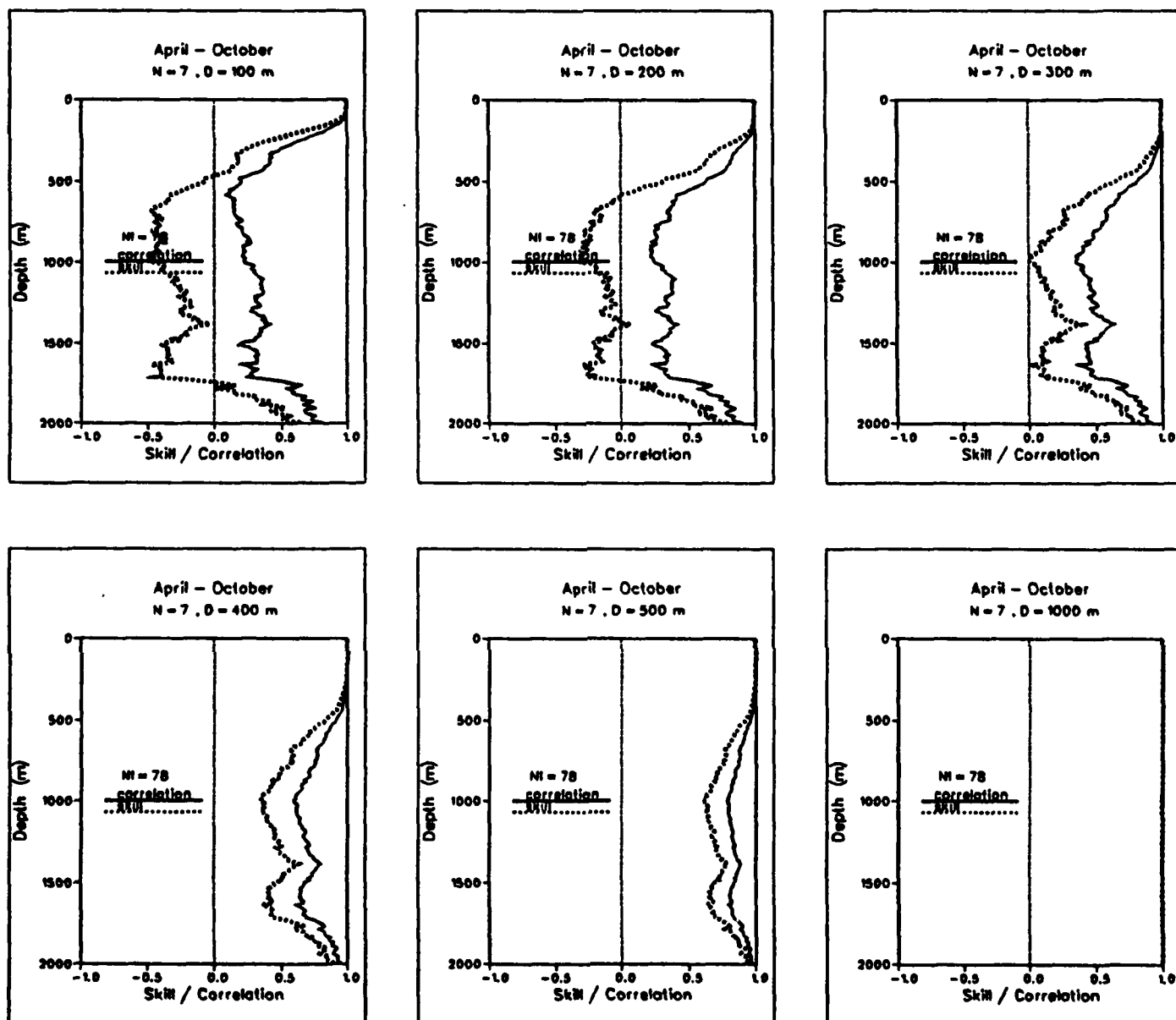


Fig. 10. A test using the culled profiles as described in the text. The results shown are the same as in Fig. 9 except that the observed profiles are replaced by the culled profiles. NI is the number of (culled) profiles used in the test.

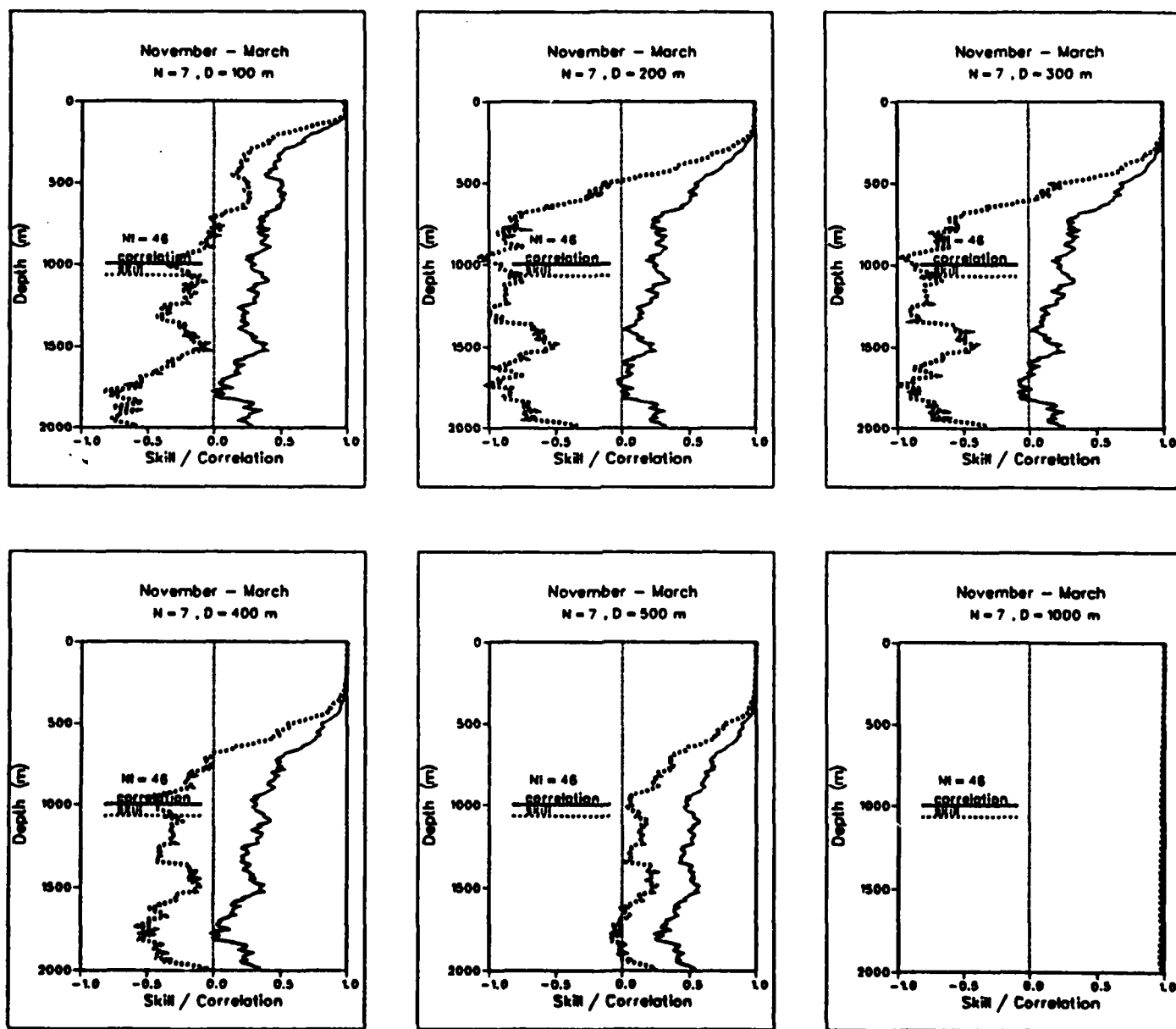


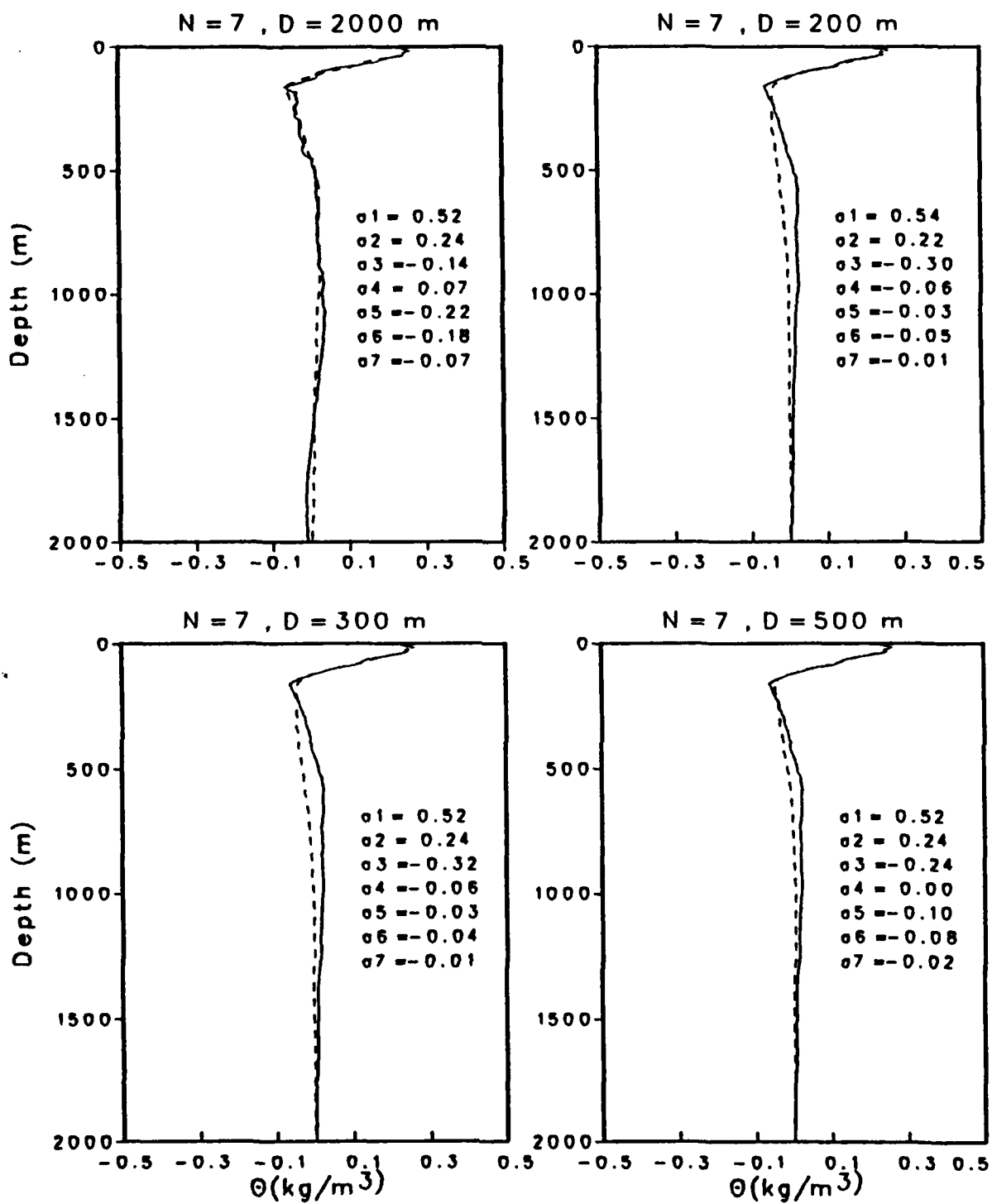
Fig. 10(b).

The way in which the estimation improves as D increases from 200 to 500 m is seen by comparing the profiles in the other three frames. In some cases the entire profile can be estimated quite accurately from only 200 m of data (Fig. 11e, f, l, p, and s), while in other cases 200 m of data is clearly inadequate (Fig. 11c, i, j, k, m, n, o, and t). Note that most of the successful cases are in the winter half-year and most of the unsuccessful cases are in the summer half-year. This is consistent with the difference in correlations shown in Fig. 7a compared to Fig. 7b.

Another point worth noting from the results in Fig. 11 is the way in which the amplitude of the different modes that make up the estimated profile changes as the depth (D) of data used in the fitting procedure is changed. In Fig. 11a for example, the amplitude of the first mode is almost the same in all four frames, indicating that it is generally well established by data down to only 200 m. This characteristic of the first mode also holds at the other locations shown in Fig. 11b, c, ... etc. It also holds to a lesser extent for the second mode, but not for the third and higher modes. This result indicates that the higher modes, unlike the lowest two modes, are not well established by shallow data alone. The lowest modes can be rather well established by fitting over a shallow depth (200 m) because they have their strongest characteristic signal in the upper 200-300 m. On the other hand, the higher modes ($n \geq 3$) have a greater part of their signal below that depth (Fig. 3). When these higher modes are active in a given profile, deeper data is needed to estimate the given profile accurately.

In most cases the estimated profile using 500 m of data matches the filtered profiles quite well. This is reflected in the rather high correlation between the filtered and

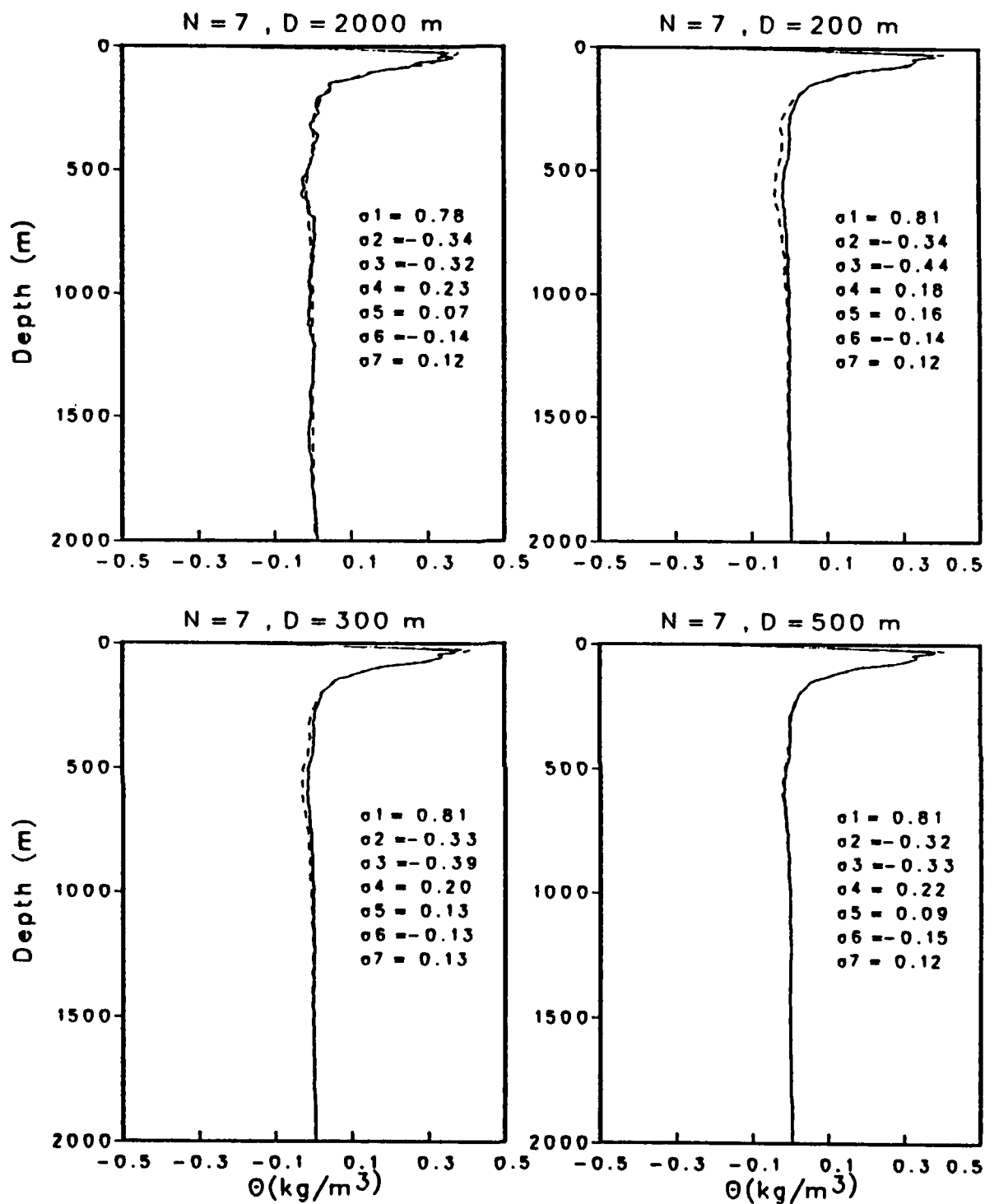
Fig. 11. The top left frame shows the observed disturbance density profile (solid) and the filtered profile (dashed) obtained from a 7-EOF reconstruction as described in the text. The other three frames show the filtered profile (solid) and the estimated filtered profile (dashed) obtained by fitting the 7 EOFs to the filtered profile above D , for $D = 200, 300$, and 500 m, respectively.



April 88

36.1N 123.5W

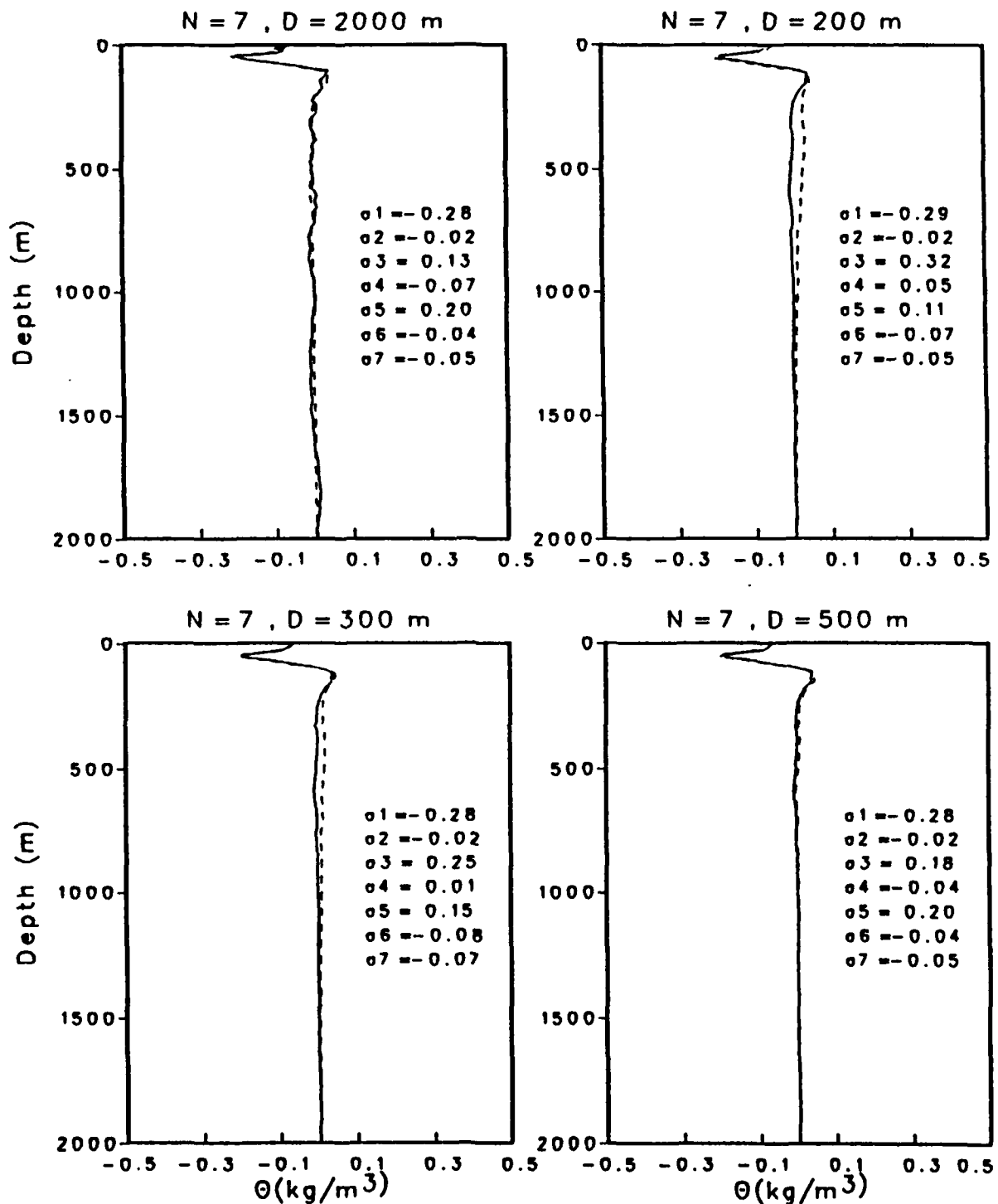
Fig. 11a



August 88

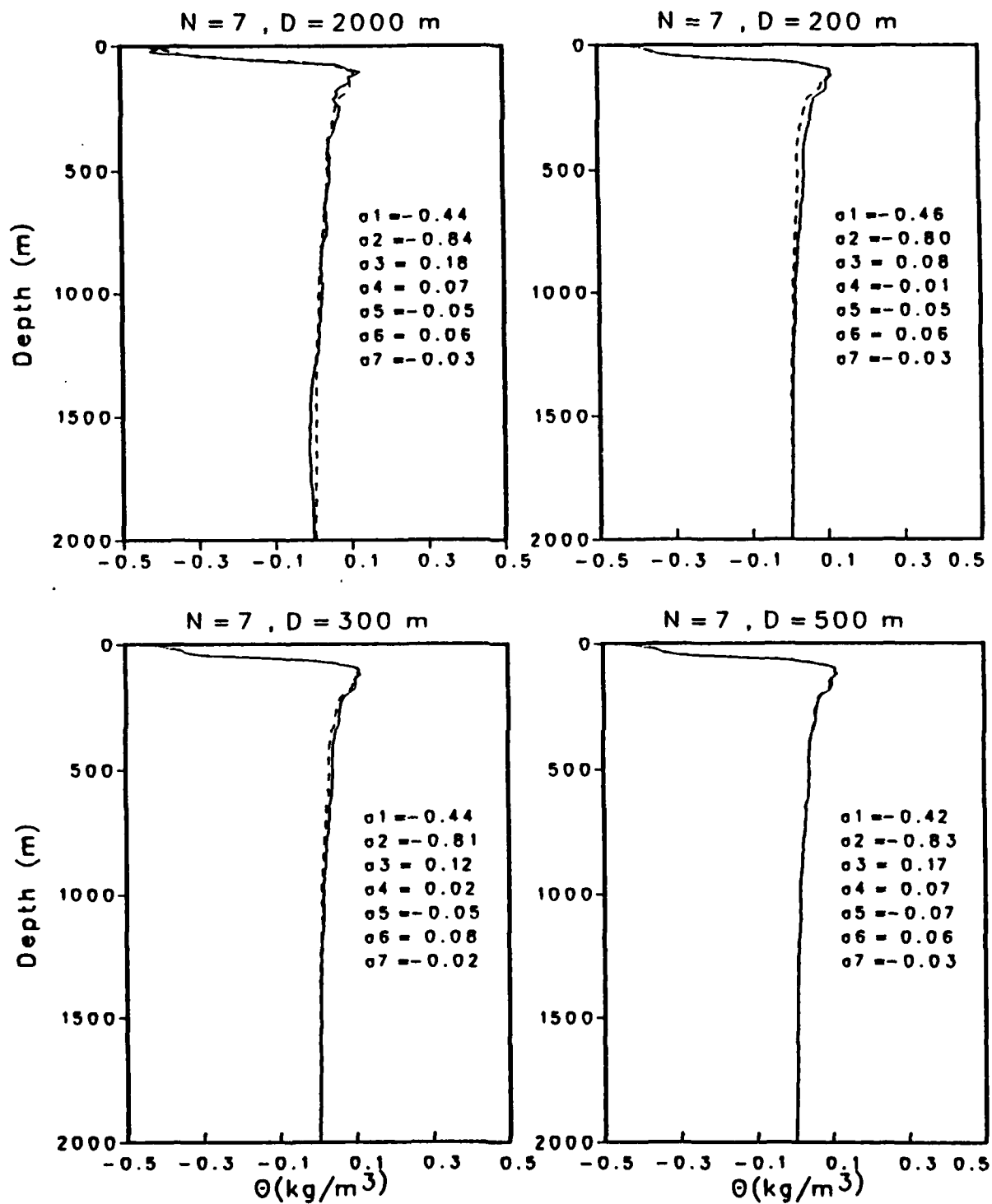
36.6N 122.5W

Fig. 11b



September 88 36.6N 122.5W

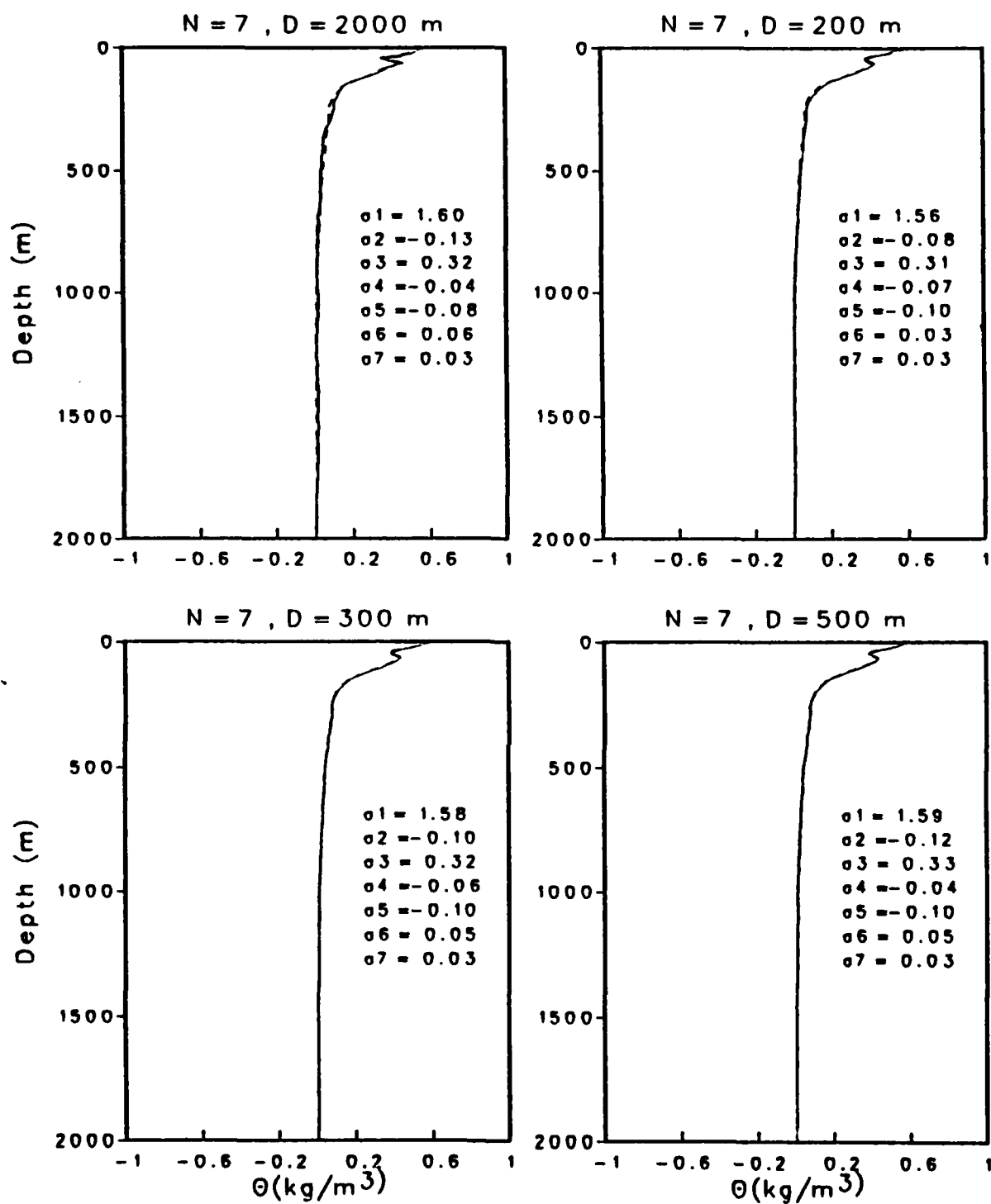
Fig. 11c



November 88

36.2N 123.3W

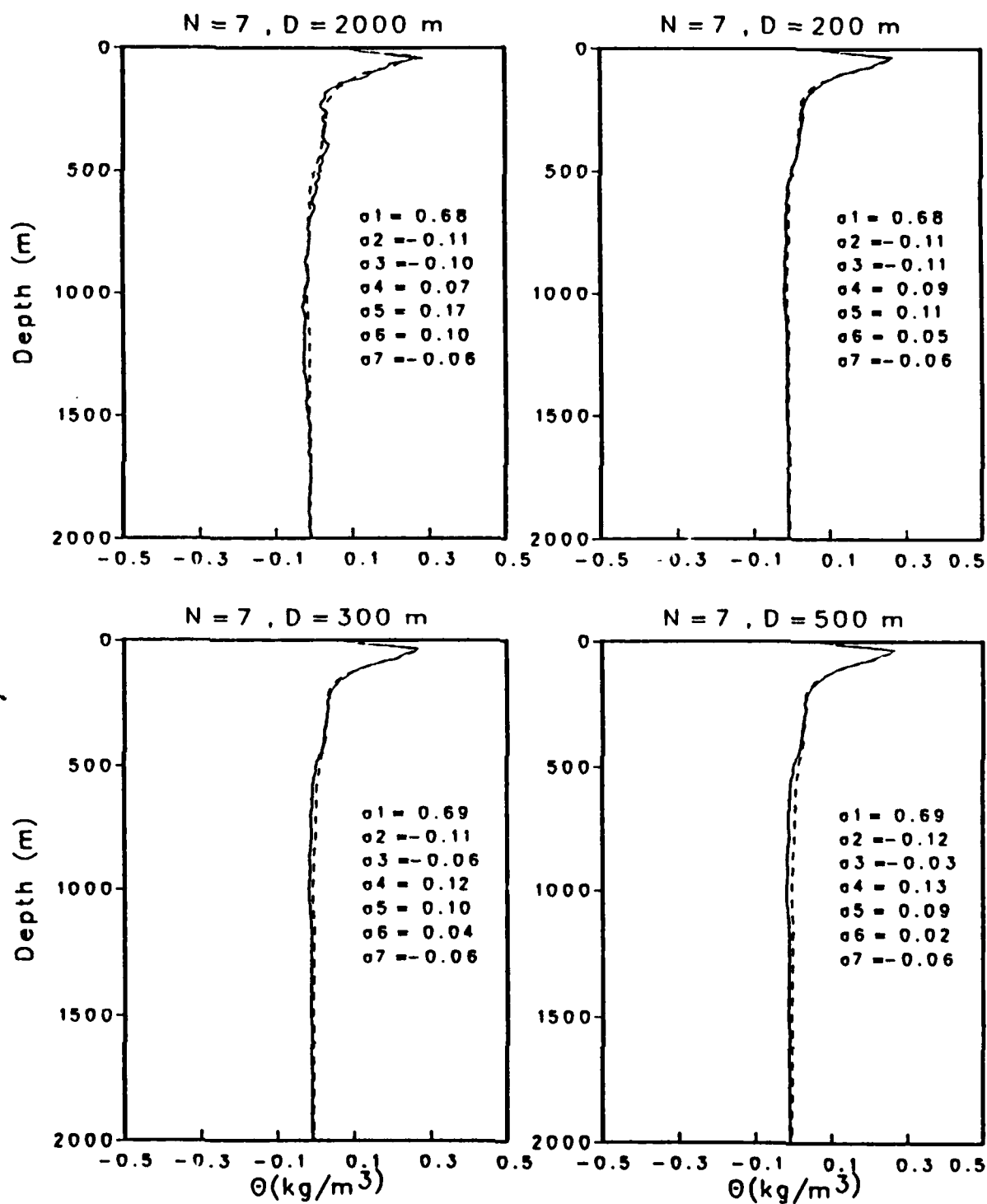
Fig. 11d



February 89

36.3N 123.2W

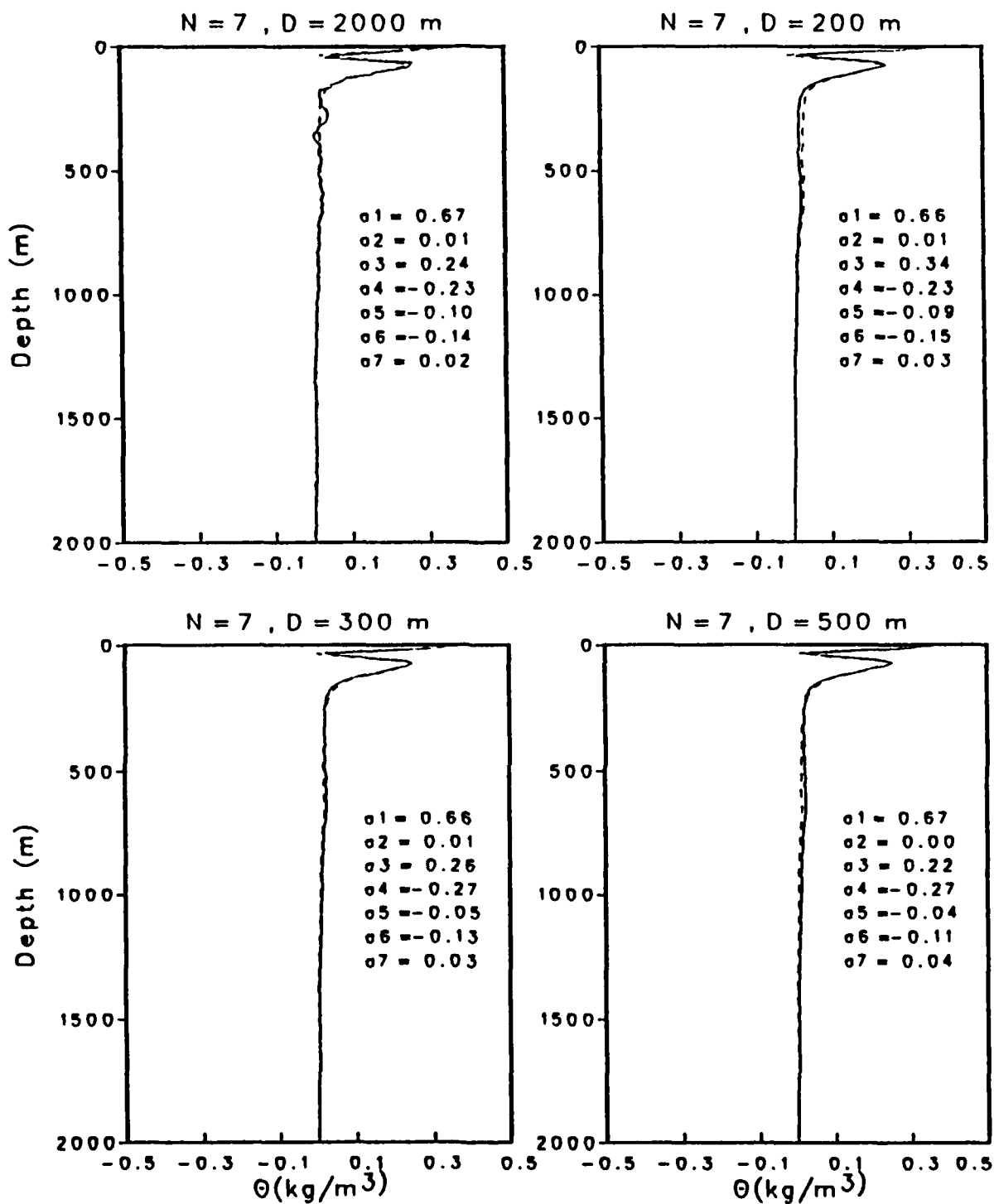
Fig. 11e



March 89

36.6N 122.5W

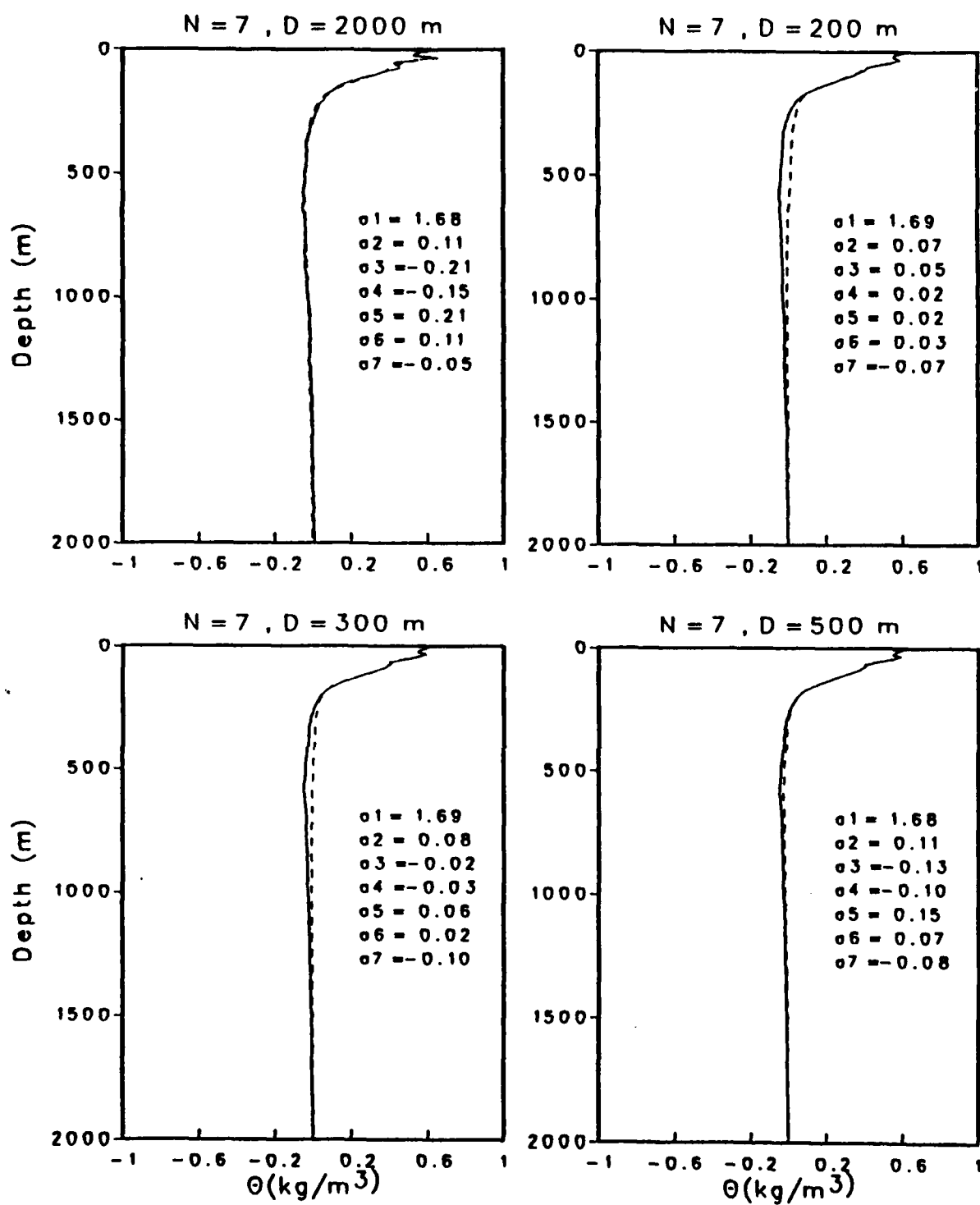
Fig. 11f



May 89

36.1N 123.5W

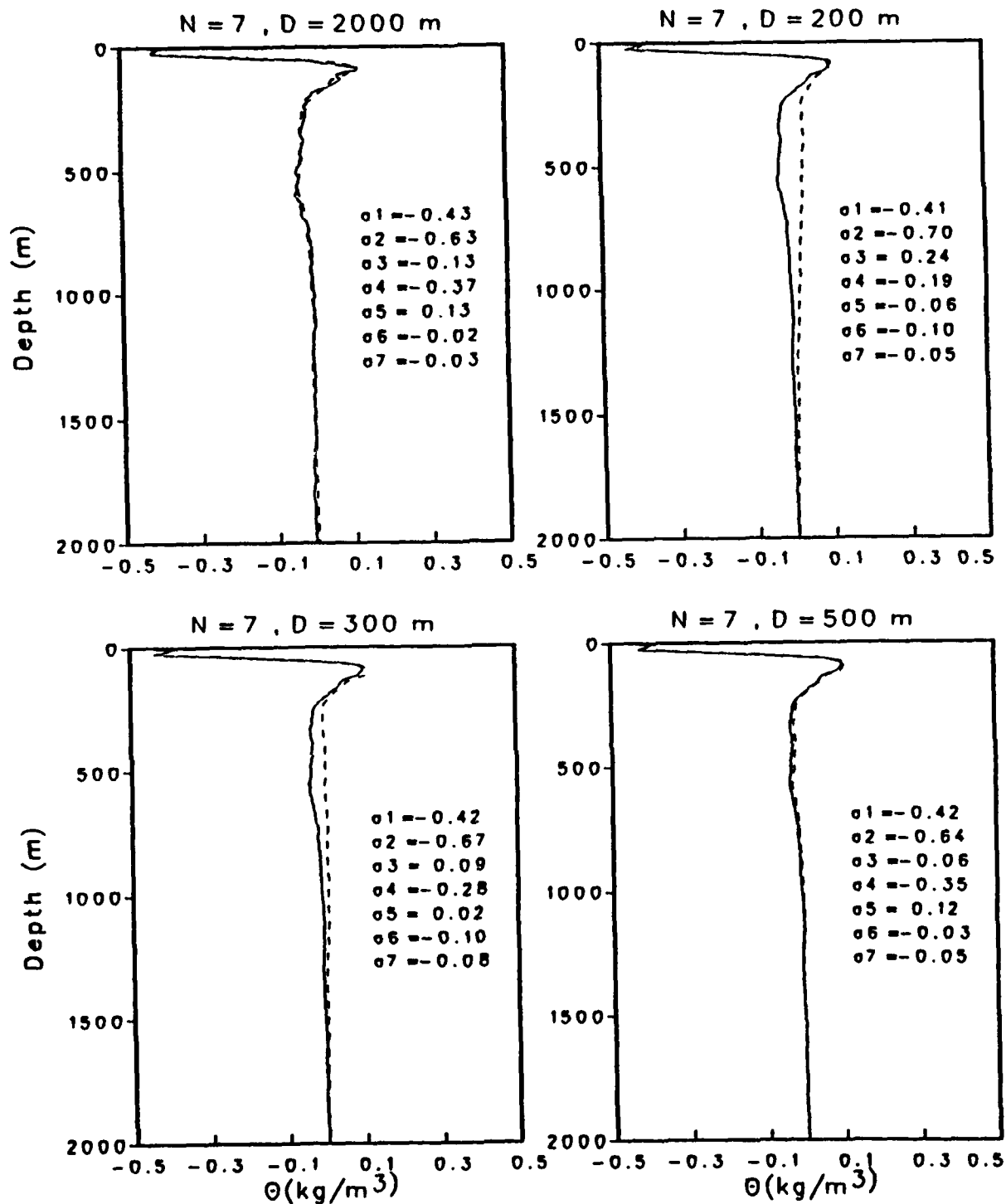
Fig. 11g



July 89

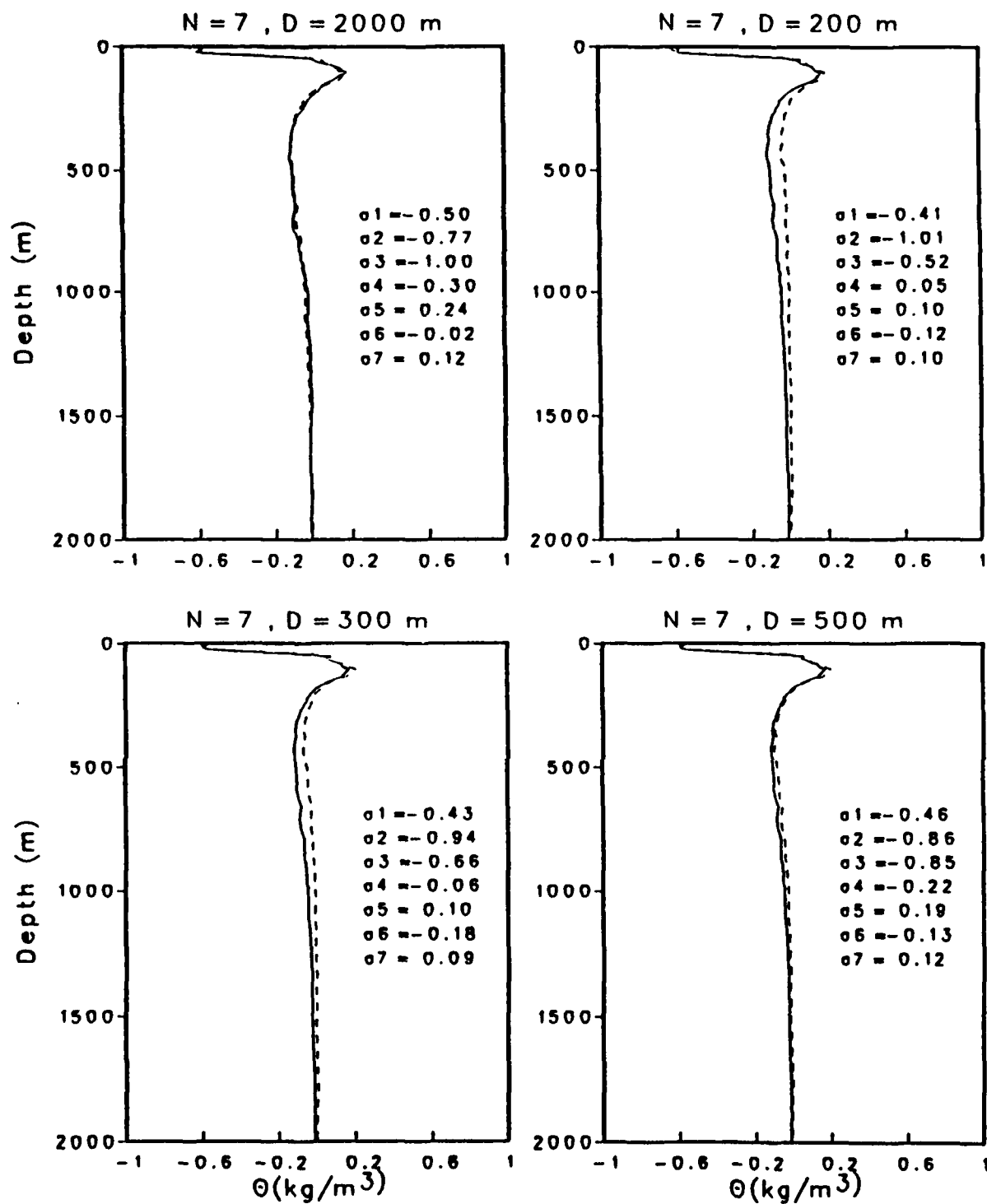
36.3N 122.5W

Fig. 11h



September 89 36.3N 122.8W

Fig. 11i



November 89

35.8N 124.2W

Fig. 11j

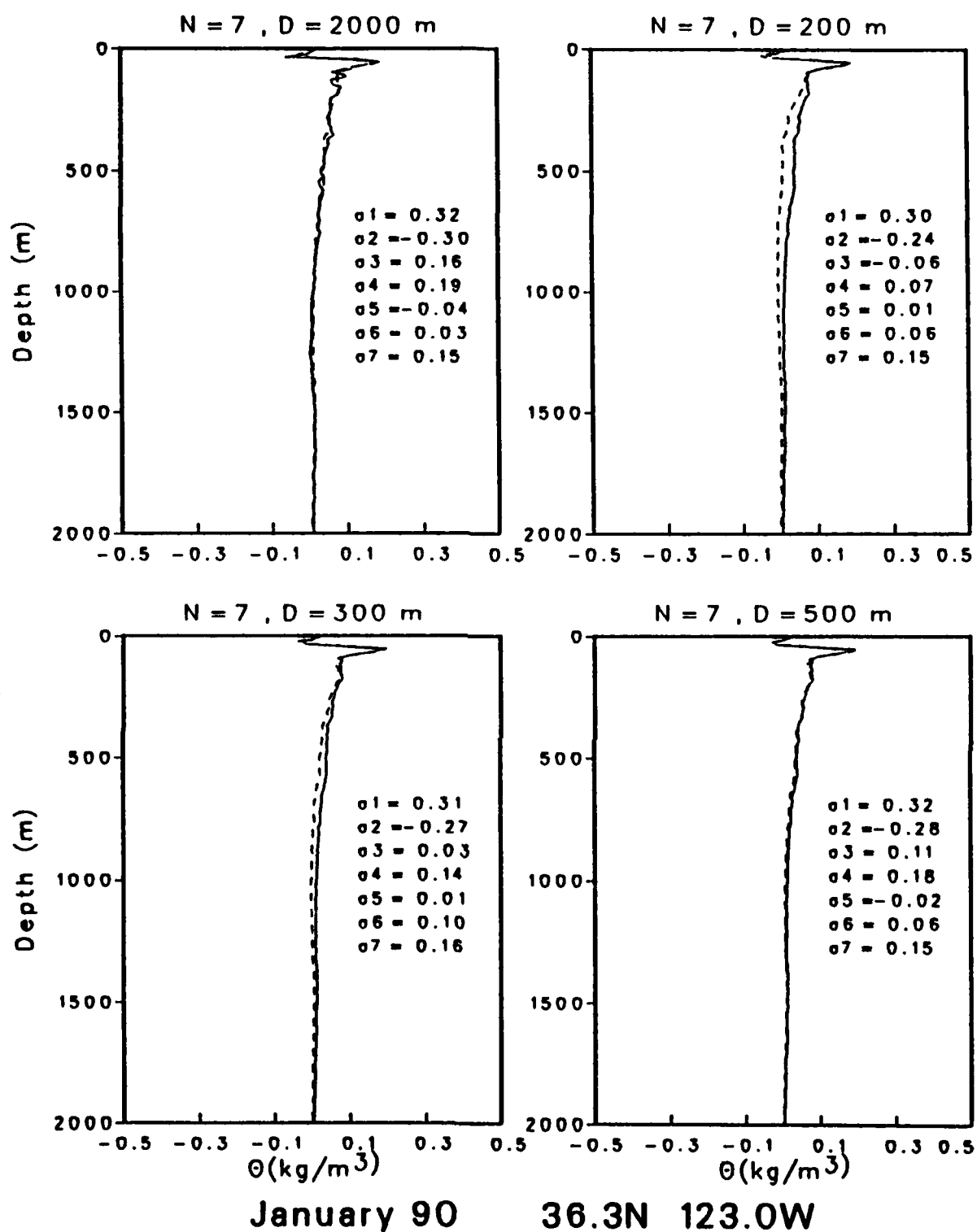
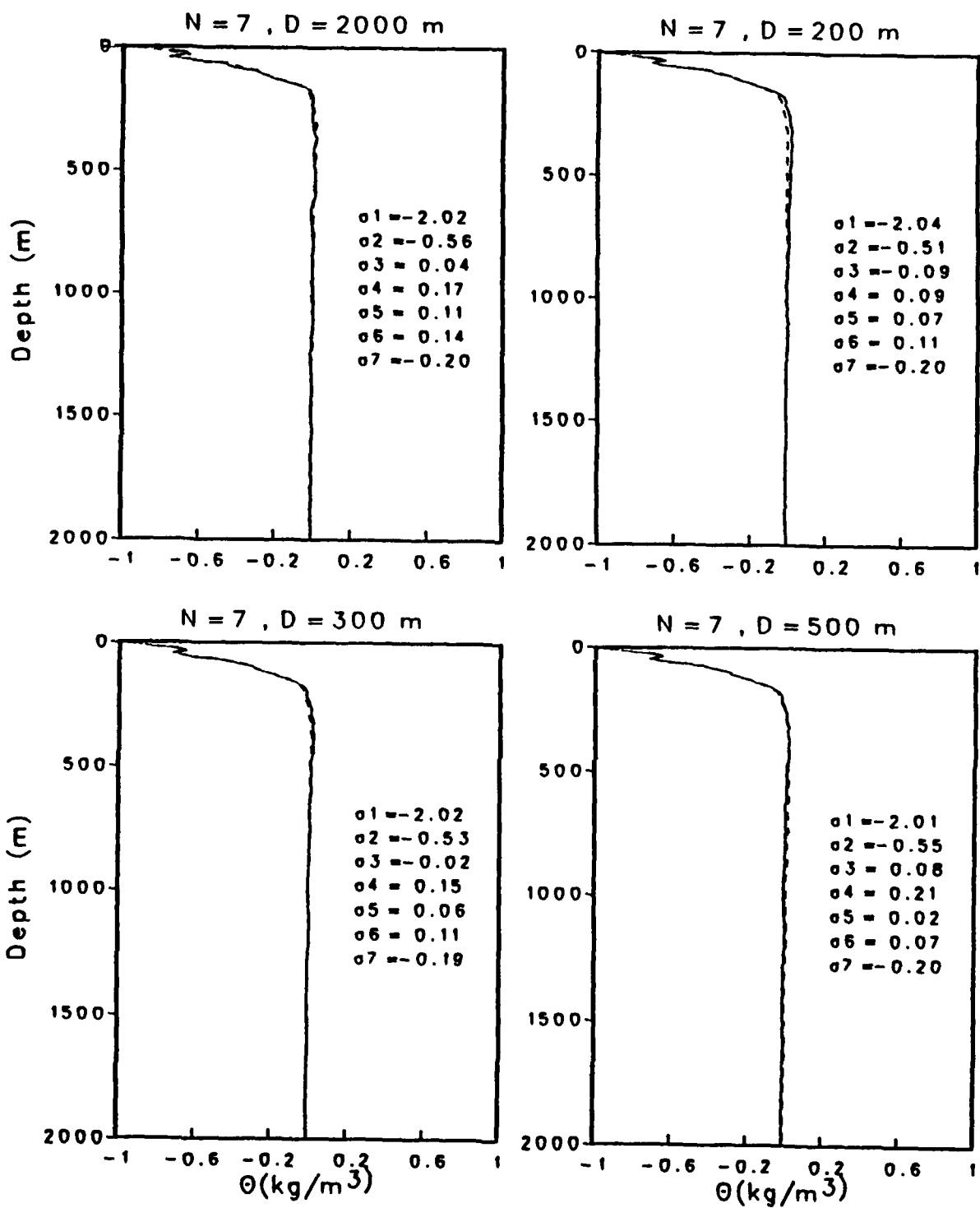


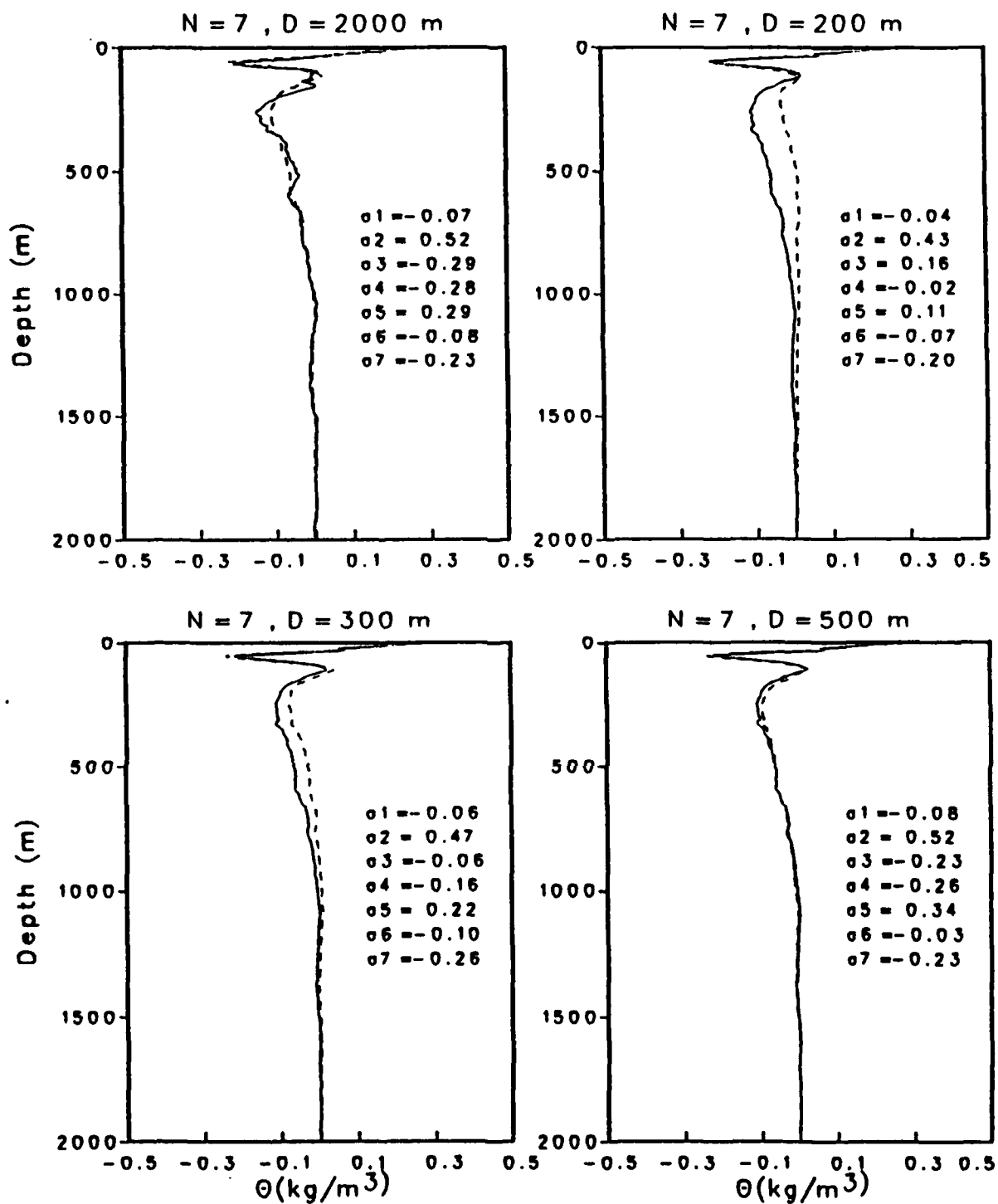
Fig. 11k



March 90

36.3N 122.9W

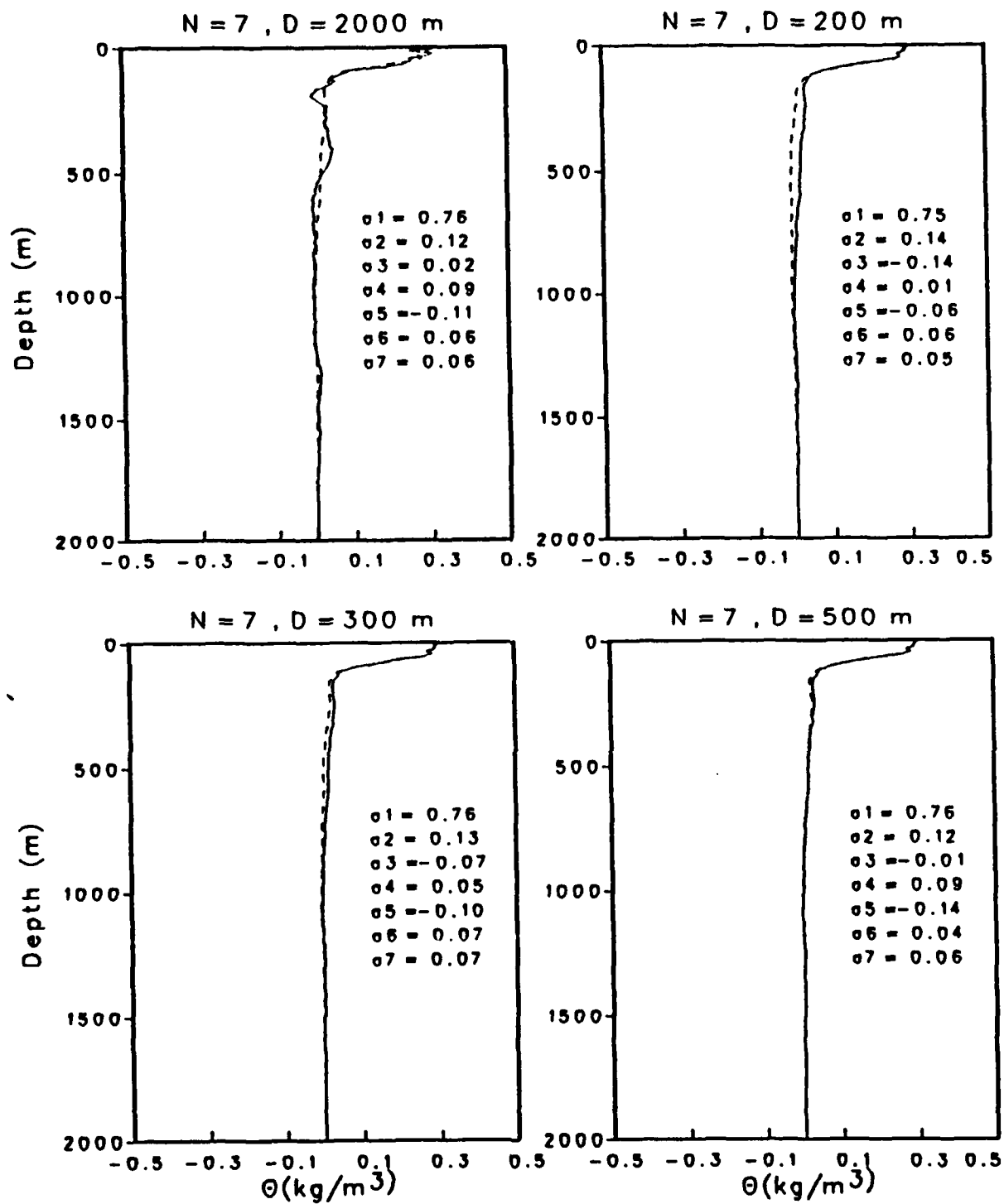
Fig. 111



May 90

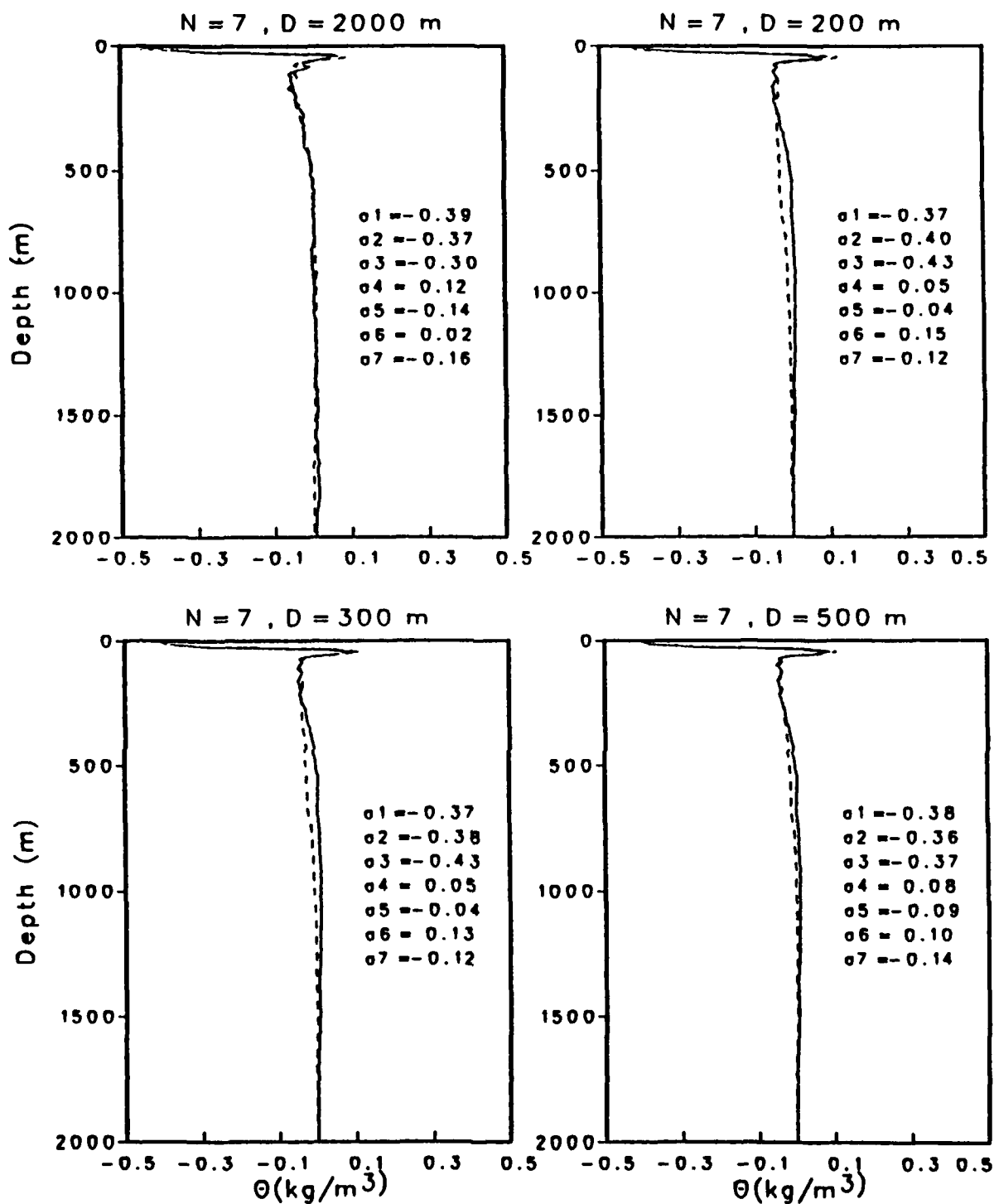
36.3N 122.9W

Fig. 11m



June 90 36.5N 122.8W

Fig. 11n



August 90 36.3N 122.6W

Fig. 11o

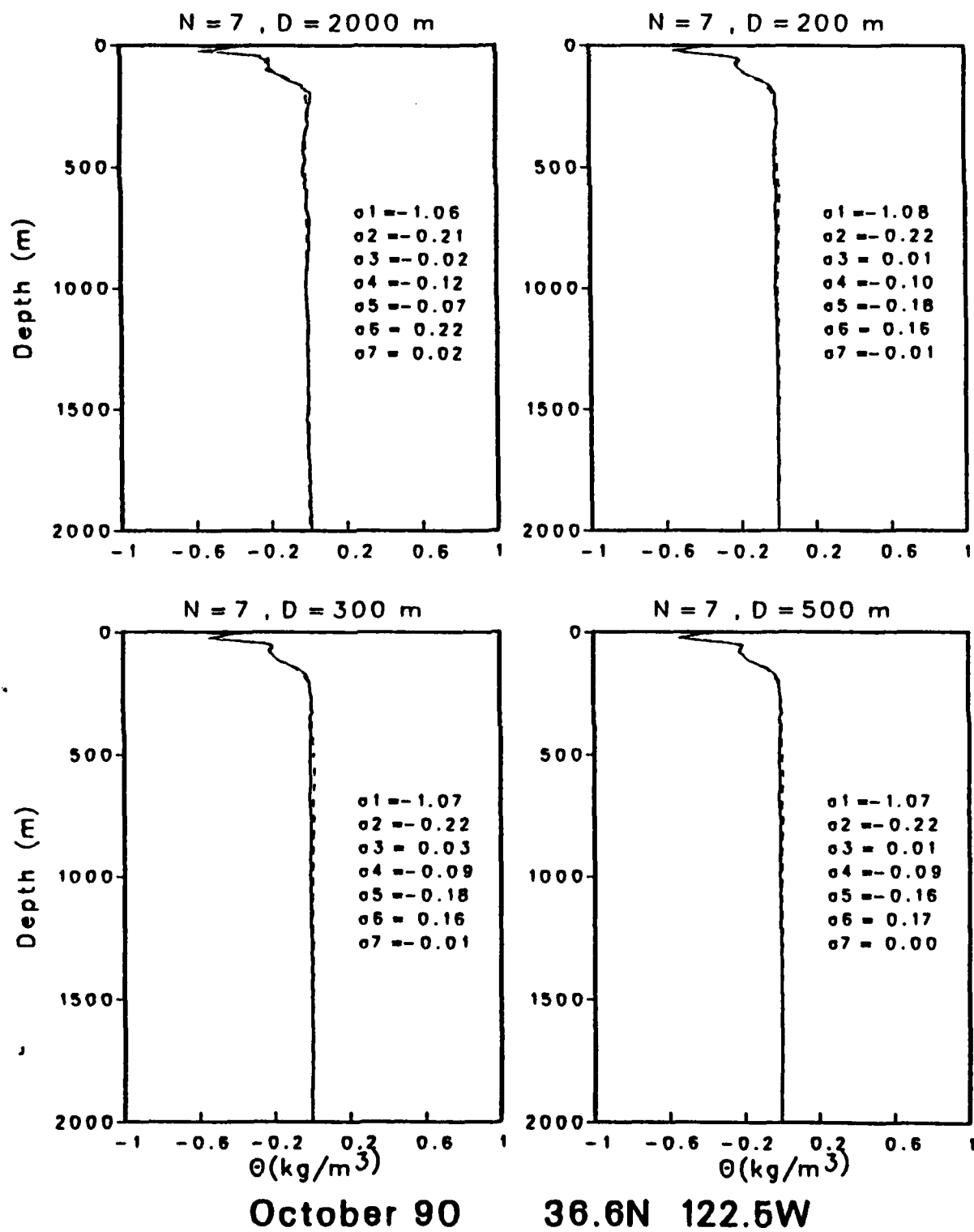
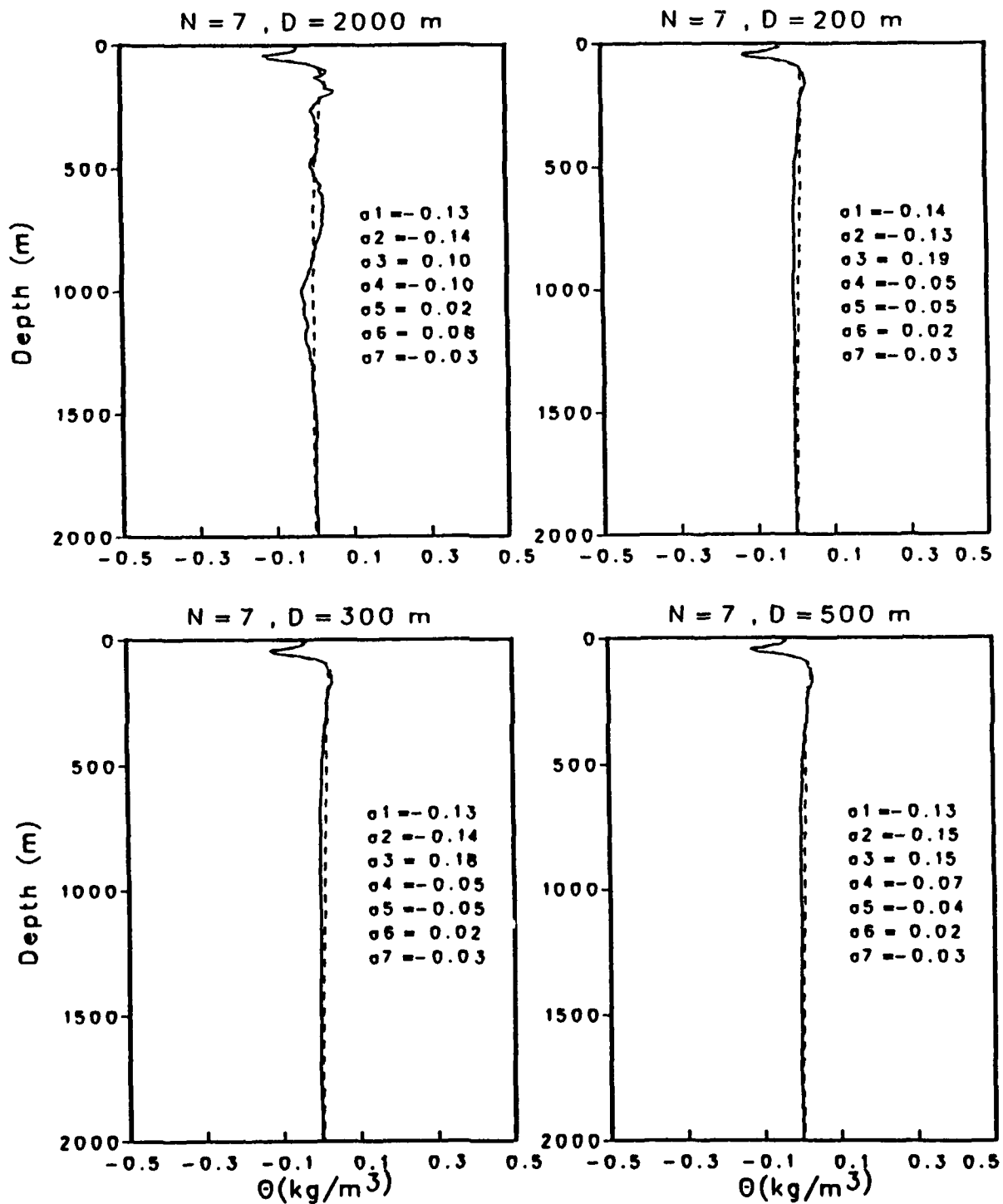
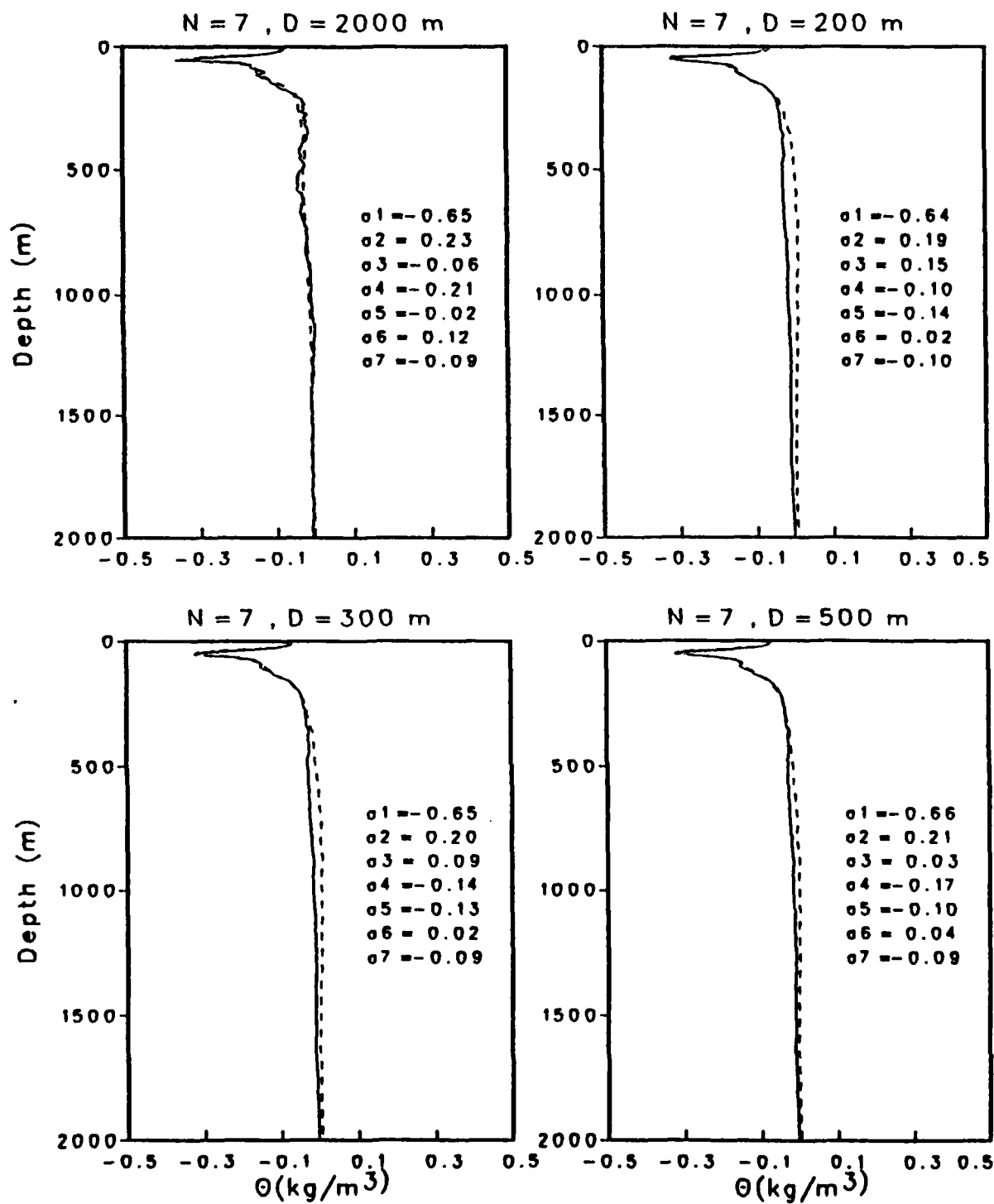


Fig. 11p



December 90 36.5N 122.8W

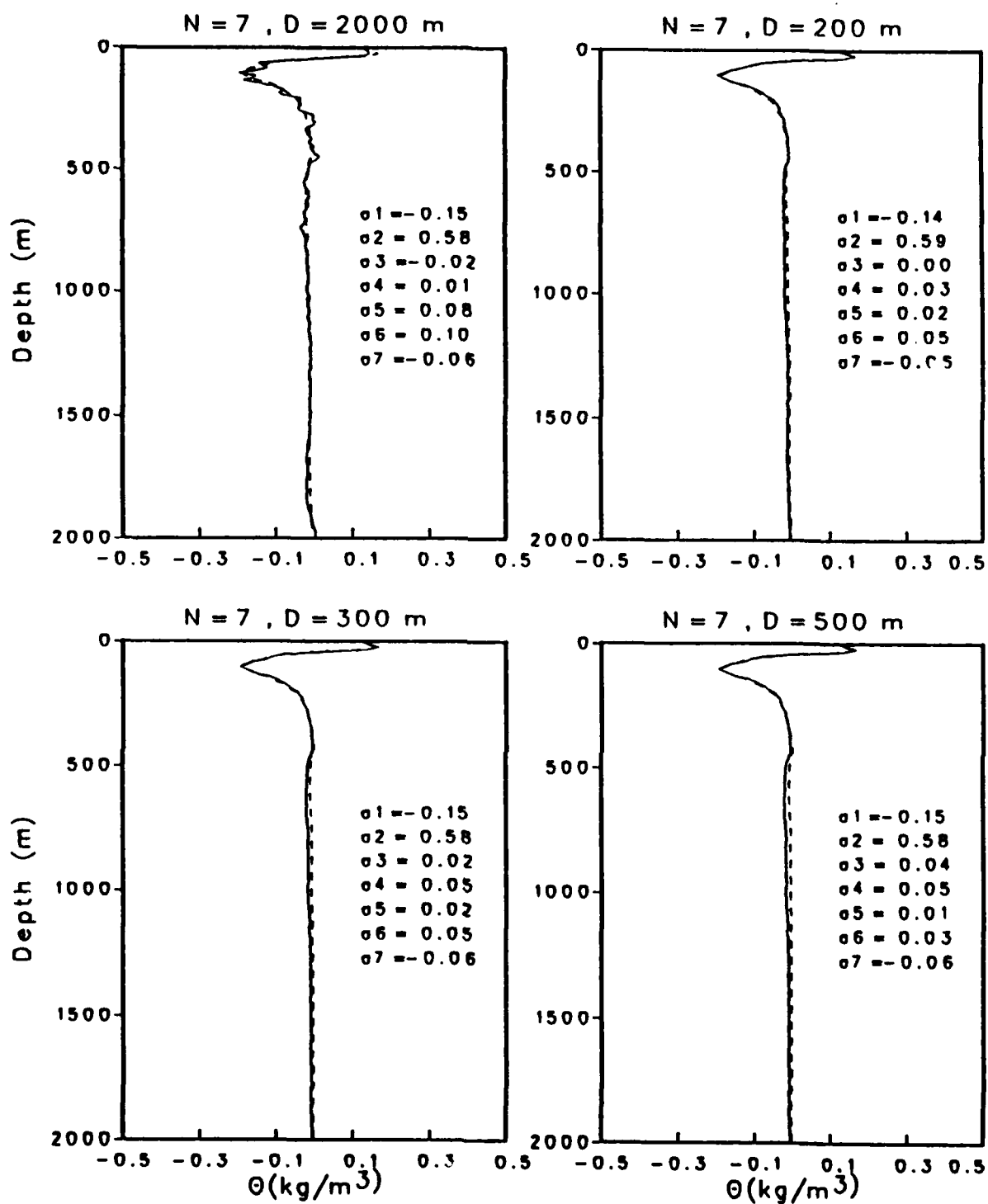
Fig. 11q



December 90

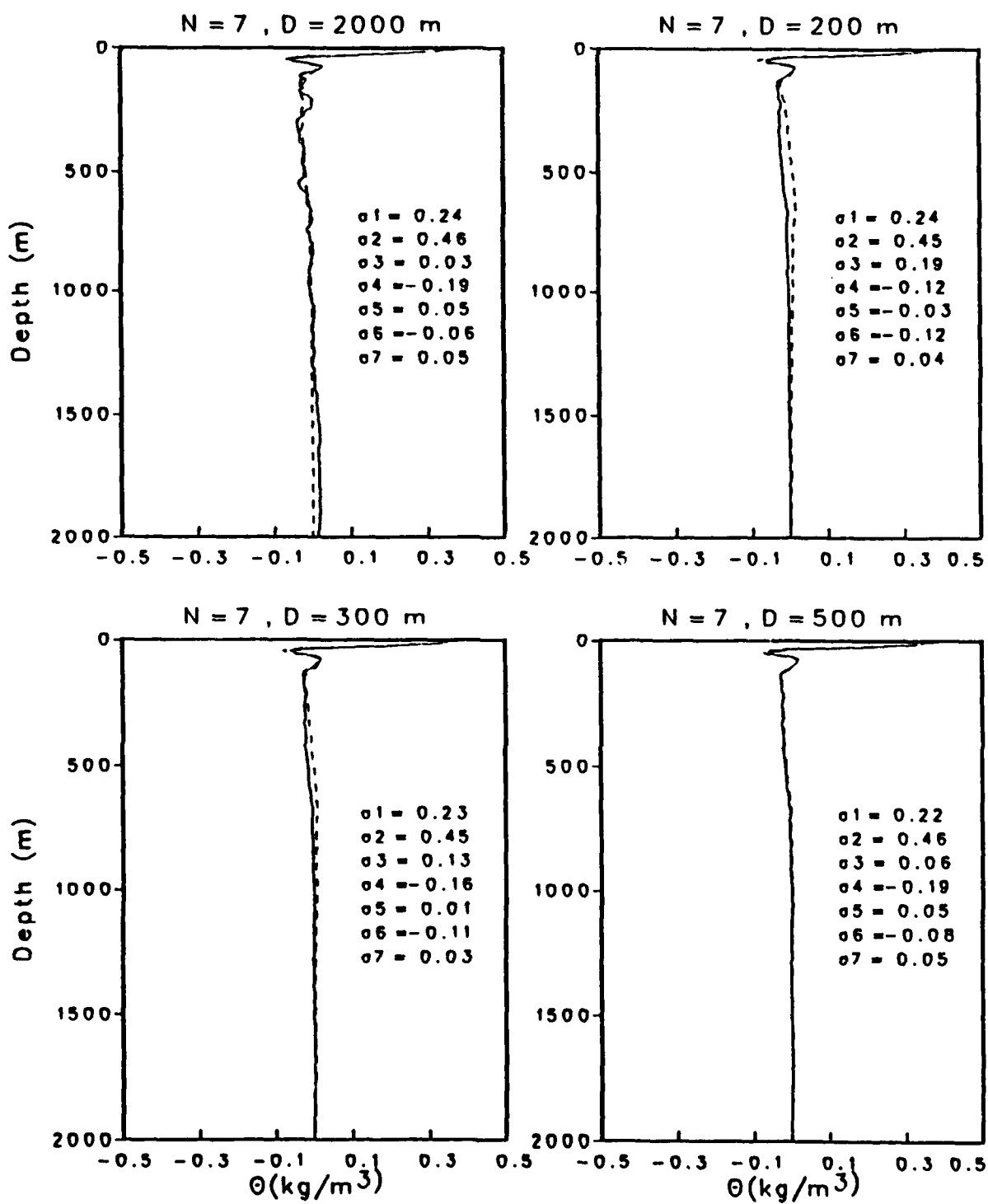
36.6N 122.5W

Fig. 11r



February 91 36.3N 122.6W

Fig. 11s



April 91 36.3N 122.6W

Fig. 11t

estimated profiles with $D = 500$ m shown in Fig. 9a, b (bottom, middle frames). Occasionally, however, even with 500 m of data, the estimation appears to miss some potentially important features (Fig. 11a, f, j, o, and g). Of course, the extent to which an estimate of the filtered profile can be considered satisfactory depends on the use to which the estimated profile will be put. The above results indicate that the method can estimate filtered profiles using data from the upper 500 m that would be satisfactory for initializing operational numerical models designed to nowcast and forecast the oceanic synoptic scale. The method might also be useful for extending historical CTD profiles (e.g., the CALCOFI data) to greater depth.

5. Summary and Conclusions

A method for extending upper ocean density profiles to the deeper ocean has been developed and tested using a large number of deep CTD stations off Point Sur, California. The method involves fitting a shallow density profile to the first N full column EOFs determined from historical data. N is the number of EOFs that are needed to represent the "signal" in the observed profiles efficiently. Our analysis, following the ideas of Preisendorfer *et al.* (1981) and Smith *et al.* (1985), resulted in $N = 7$ for our data. The EOFs found in this study are quite similar to those described by Chelton (1980), Rienecker *et al.* (1987) and Bray and Greengrove (1993) for the nearby California Current region. The first mode is due to fluctuations in the baroclinic structure associated with the equatorward vertical shear of the California Current in the main pycnocline, while the second mode appears to represent a response in the mixed layer and the pycnocline to variations in alongshore wind stress. The third and fourth modes have deeper structures. All of these

modes make important contributions to the success of the vertical extension method.

When the vertical extension method is tested against the observed profiles the results are moderately successful (Fig. 7). Profiles to depths shallower than 500 m can be extended to 500 m with an over all correlation and skill that depends on the time of year as well as the depth of the profiles. For example, profiles to 300 m can be extended to 500 m with noticeably better correlation than ones to only 200 m. In all cases the extensions from depths shallower than 500 m to depths greater than 500 m are notably more successful in winter than in summer. In all cases the estimated profiles correlate better with filtered (noise-free) profiles, reconstructed from the first 7 EOFs, because the method cannot estimate variability associated with vertically incoherent noise. The improved correlations due to removing such noise is significant at all depths below D in winter, but only below about 1000 m in summer.

The above results raise important questions about the generality of the vertical extension method, and whether it would be successful in other geographical regions. The success of the method rests on its ability to detect, and differentiate between, the EOF modes in the region of interest from only a limited amount of upper ocean data. As such, its success depends on the distinctive shapes of the different modes and most importantly on whether the modes have significant signals at depth. On the basis of these considerations we expect the method would be equally successful in all the dynamically active parts of the world ocean where the internal density fluctuations are associated with moderate to deep baroclinic structures similar to those that exist in the California Current off Point Sur.

Acknowledgements. We are grateful to Leonard Walstad, Michele Rienecker, and Dudley

Chelton, as well as our NPS colleagues J.-M. Chen and Pat Harr for especially valuable discussions and input on the topic of this paper. This work was sponsored by the Applied Oceanography Division (Code 124) of the Office of Naval Research and the Naval Postgraduate School whose support is gratefully acknowledged. Ms. Penny Jones typed and revised this paper.

References

- Bray, N. A., and C. L. Greengrove, 1993: Circulation over the shelf and slope off Northern California. J. Geophys. Res., **98**, 18119-18145.
- Chelton, D. B., Jr., 1980: Low frequency sea level variability along the west coast of North America. Ph.D. dissertation, Scripps Instit. of Oceanogr., La Jolla, CA.
- Hurlburt, H. E., D. N. Fox, and E. J. Metzger, 1990: Statistical inference of weakly-correlated subthermocline fields from satellite altimeter data. J. Geophys. Res., **95** (C7), 11375-11409.
- Lentz, S. J., 1987: A description of the 1981 and 1982 spring transitions over the Northern California shelf. J. Geophys. Res., **92** (C2), 1545-1567.
- Mellor, G. L., and T. Ezer, 1991: A Gulf Stream model and an altimetry assimilation scheme. J. Geophys. Res., **96** (C5), 8779-8795.
- North, G. R., T. L. Bell, R. F. Cahalan, and F. J. Moeng, 1982: Sampling errors in the estimation of empirical orthogonal functions. Mon. Wea. Rev., **110**, 699-706.
- Preisendorfer, R. W., F. W. Zweirs, and T. P. Barnett, 1981: Foundations of principal component selection rules. SIO Ref. Series 81-4, Scripps Inst. of Oceanography, 192 pp.
- Rienecker, M. M., C.N.K. Mooers, and A. R. Robinson, 1987: Dynamical interpolation and forecast of the evolution of mesoscale features off Northern California. J. Phys. Oceanogr., **17**, 1189-1213.
- Smith, J. A., 1984: Empirical and dynamic modes in the CCS. NPS Tech. Rep. NPS 68-84-003, Naval Postgraduate School, 42 pp.

- Robinson, A. R., M. A. Spall, and N. Pinardi, 1988: Gulf Stream simulations and the dynamics of ring and meander processes. J. Phys. Oceanogr., 18, 1811-1853.
- Smith, J. A., C.N.K. Mooers, and A. R. Robinson, 1985: Estimation of quasi-geostrophic modal amplitudes from XBT/CTD survey data. J. Atmos. Ocean. Tech., 2, 491-507.
- Strub, P. T., J. S. Allen, A. Huyer, and R. L. Smith, 1987: Large scale structure of the spring transition in the coastal ocean off Western North America. J. Geophys. Res., 92 (C2), 1527-1544.
- Tisch, T. D., S. R. Ramp, and C. A. Collins, 1992: Observations of the geostrophic current and water mass characteristics off Point Sur, California from May 1988 through November 1989. J. Geophys. Res., 97 (C8), 12535-12555.

DISTRIBUTION LIST

	<u>No. Copies</u>
Defense Technical Information Center Cameron Station Alexandria, VA 22304-6145	2
Library (Code 0142) Naval Postgraduate School Monterey, CA 93943	2
Dean of Research (Code 08) Naval Postgraduate School Monterey, CA 93943	1
Dr. Robert L. Haney (Code MR/Hy) Chairman, Department of Meteorology Naval Postgraduate School Monterey, CA 93943-5114	20
Dr. Curtis A. Collins (Code OC/Co) Chairman, Department of Oceanography Naval Postgraduate School Monterey, CA 93943	1
Mr. Robert A. Hale (Code MR/HI) Department of Meteorology Naval Postgraduate School Monterey, CA 93943-5114	1
Mr. Robert Peloquin Applied Oceanography and Acoustics Division ONR Code 124 800 N. Quincy St. Arlington, VA 22217-5000	1
Dr. Manuel Fiadeiro Physical Oceanography ONR Code 322 PO 800 N. Quincy St. Arlington, VA 22217-5000	1

Commanding Officer Naval Oceanography Command Stennis Space Center, MS 39529-5000	1
Commanding Officer Naval Oceanographic Office Stennis Space Center, MS 39529-5001	1
Commanding Officer Fleet Numerical Meteorology and Oceanography Command Naval Postgraduate School Monterey, CA 93943	1
Superintendent Naval Research Laboratory, Stennis Stennis Space Center, MS 39529	1